A Mass Conservative Streamline Tracking Method for Three Dimensional CFD Velocity Fields

A thesis submitted to the University of the South Pacific for the Partial fulfillment for the degree of

Master of Science

(MSc. Mathematics)

By

Roslyn Preetika Singh

Abstract

Fluid flow visualization methods have attracted global attention from different areas such as computer science and engineering. One of the methods of visualizing fluid flow is the construction of streamlines, which are lines that are everywhere tangential to the fluid velocity fields. Streamline visualization is an important instrument for exploring the properties of a fluid velocity field.

In three dimensions a CFD velocity field is defined at discrete locations and it is assumed that this discrete velocity field is an approximation to a continuous mass conservative velocity field within the same domain. However, most interpolations of the velocity fields over each cell in a mesh are mathematical approximations and the resulting fields do not always satisfy the law of mass conservation.

In this thesis I have simplified the three-dimensional mass conservative streamline tracking method given in [6] for CFD velocity fields without further data available. Such CFD velocity fields may be obtained by the measurements of devices, for example, measured wind velocity fields. This result is also an extension of an existing two-dimensional result for the same CFD velocity field in [7].

The performance of the new algorithm is simpler and quicker than the old algorithm [6]. The accuracy of this new method as compared to the exact streamline has been shown through two examples for analytical velocity fields.

The discussion for streamline tracking method in this thesis is for incompressible flows but the method can also be used for compressible steady flows by replacing CFD velocity fields with CFD momentum fields.

A full explanation of this simplification process is carried out in Chapter 4 of this thesis. The simplified process is less time consuming and highly accurate.

Declaration

I hereby declare that the ideas, results, analyses and conclusions reported in this thesis are entirely my own effort, except where otherwise acknowledged. I also declare that the work is original and has not been previously submitted for any other award.

Roslyn Preetika Singh

Acknowledgement

I would like to extend a special thanks to my supervisor, Dr Zhenquan Li, for his guidance, support and patience throughout my masters program. I am also grateful to him for providing me with the opportunity to conduct this study and for directing me and encouraging me in preparation of this thesis.

I would also like to thank The University of the South Pacific and School of Computing, Information and Mathematical Science for providing me with the resources during my study.

Finally I wish to thank my family for their love and emotional support, as well as understanding and patience.

Contribution

A part of the research in this thesis has been published in the *Journal of Flow Visualization and Image Processing*, Volume 14, pp. 107-120, 2007.

Contents

Chapter 1 Introduction

This Chapter briefly describes some basic concepts in Computational Fluid Dynamics (CFD) and flow visualization.

Let us start by introducing what CFD stands for.

Computational: having to do with computers.

Fluid: a substance, as a liquid or gas, that is capable of flowing and that changes its shape at a steady rate when acted upon by a force tending to change its shape.

Dynamics: The forces and motions that characterize a system.

Hence CFD is a computational technology that assists in studying the dynamics of fluids. CFD software enables you to simulate flows of gases and liquids, heat and mass transfer, moving bodies, multiphase physics, chemical reaction, fluid-structure interaction and acoustics through computer modeling.

Now let us have a closer look at fluid and its properties.

1.1 Properties of Fluid

A fluid is defined as a substance that continually deforms under shear stress. Generally they are classified as either liquids or gases. The behavior of fluids can be described by the Navier–Stokes equations—a set of partial differential equations which are based on:

- continuity (conservation of mass).
- conservation of linear momentum.
- conservation of angular momentum.
- conservation of energy.

The study of fluids is fluid mechanics, which is subdivided into fluid dynamics and fluid statics depending on whether the fluid is in motion.

1.2 Fluid Dynamics

Fluid dynamics deals with fluid flow. Fluid dynamics has a wide range of applications, including calculating forces and moments on aircraft, determining the mass flow rate of petroleum through pipelines, predicting weather patterns, understanding nebulae in interstellar space and reportedly modeling fission weapon detonation. Some of its principles are even used in traffic engineering, where traffic is treated as a continuous fluid.

Fluid dynamics offers a systematic structure that underlies these practical disciplines and that embraces empirical and semi-empirical laws, derived from flow measurement, used to solve practical problems. The solution of a fluid dynamics problem typically involves calculation of various properties of the fluid, such as velocity, pressure, density, and temperature, as functions of space and time.

1.3 Equations of Fluid Dynamics

The fundamental equations describing fluid dynamics are based on conservation laws, specifically:

- conservation of mass.
- conservation of linear momentum (also known as Newton's Second Law of Motion).
- conservation of energy (also known as First Law of Thermodynamics).

These are based on classical mechanics and are modified in quantum mechanics and general relativity.

In addition to the above, fluids are assumed to obey the *continuum assumption*. As we all know fluids are composed of molecules, however, the continuum assumption considers fluids to be continuous, rather than discrete. Consequently, properties such as density, pressure, temperature, and velocity are taken to be well-defined at infinitesimally small points, and are assumed to vary continuously from one point to another. The fact that the fluid is made up of discrete molecules is ignored.

For fluids which are sufficiently dense to be a continuum, do not contain ionized species, and have velocities small in relation to the speed of light, the momentum equations for Newtonian fluids are the Navier-Stokes equations, which is a non-linear set of differential equations that describes the flow of a fluid whose stress depends linearly on velocity gradients and pressure. The equations do not have a general closed-form solution, so they are primarily of use in Computational Fluid Dynamics. The equations can be simplified in a number of ways, all of which make them easier to solve. Some of them allow appropriate fluid dynamics problems to be solved in closed form.

1.4 Incompressible and Steady Flow

In this thesis we have assumed that the fluid flow involved is steady and incompressible. All fluids are compressible to some extent, i.e. changes in pressure or temperature, will result in changes in density. However, in this thesis we assume that

the changes in pressure and temperature are sufficiently small that the changes in density are negligible. So the flow is modeled as an incompressible flow. Mathematically, incompressibility is expressed by saying that the density ρ of a fluid parcel does not change as it moves in the flow field.

Steady flow is defined as fluid flow where at any one point the conditions are constant with respect to time. Hence all the time derivatives of a flow field vanish.

In this thesis, we introduce a simplified streamline tracking method for steady or impressible fluid flows. The following section shows some common knowledge relate to flow visualization.

1.5 Flow Visualization

Flow visualization in fluid dynamics is used to make the flow patterns visible, in order to get qualitative or quantitative information on them.

Fluid flow is characterized by a velocity vector field in three-dimensional space, within the framework of continuum mechanics. **Streamlines, streaklines and pathlines** are field lines resulting from this vector field description of the flow. For a steady flow (see below), the three are the same as shown in Fig. 1.1. While for a non-steady flow they are generally different.

- **Streamlines** are a family of curves that are instantaneously tangent to the velocity field of the flow as shown in Fig. 1.2.

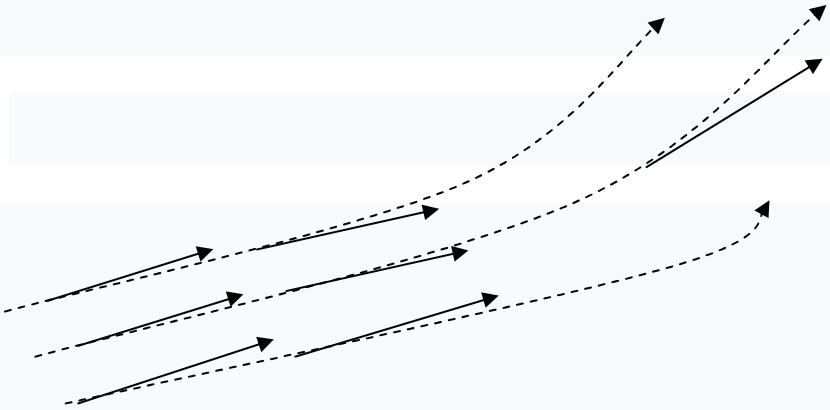

Fig. 1.1 Streamlines

A streamline is a line which is tangential to the velocity field at every point in the flow at any given instant. The definition leads to the following equation for streamlines:

$$\frac{dx}{u} = \frac{dy}{v} = \frac{dz}{w},$$

where (u,v,w) is the velocity field, u, v, and w are the components in x-direction, y-direction, and z-direction, respectively.

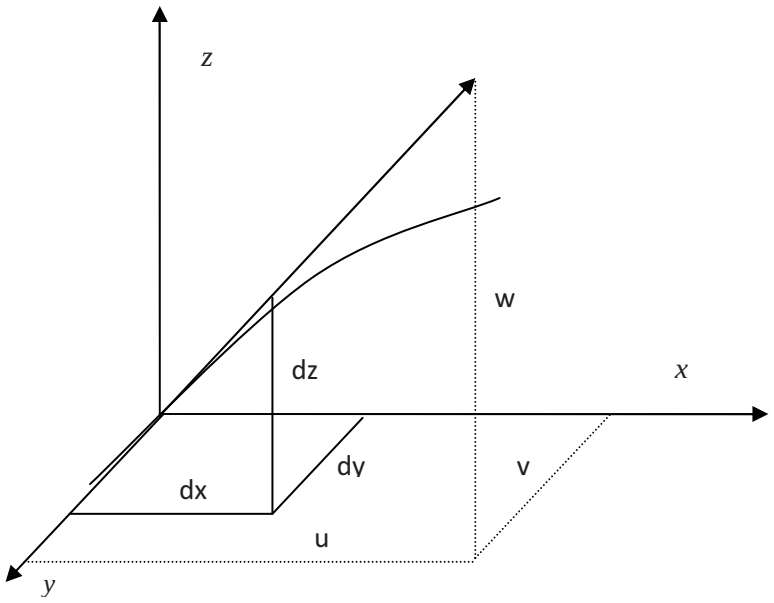

Fig. 1.2 Streamline Definition

- **Streaklines** are the locus of points of all the fluid particles that have passed continuously through a particular spatial point in the past. Dye steadily injected into the fluid at a fixed point extends along a streakline as shown in Fig. 1.3.

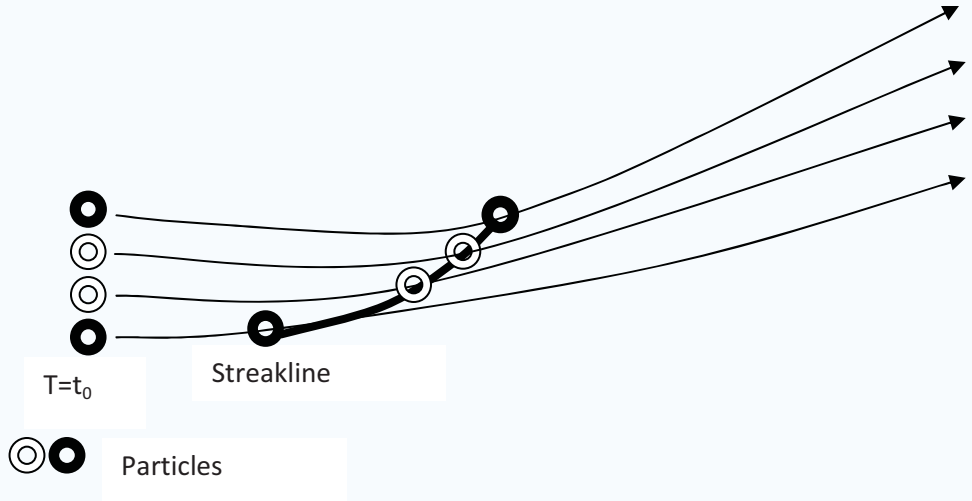

Fig. 1.3 Streaklines

- **Pathlines** are the trajectories that individual fluid particles follow as shown in Fig. 1.4.

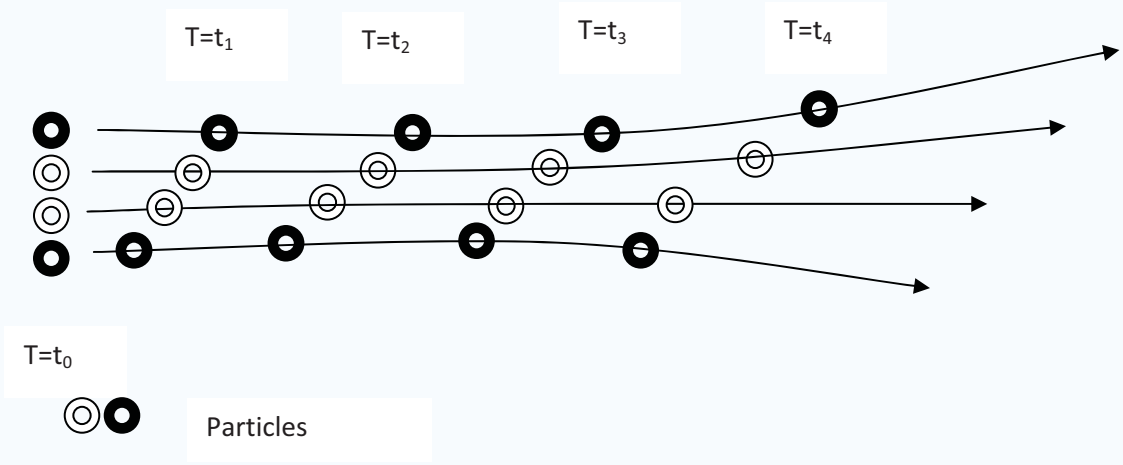

Fig. 1.4 Pathlines

- **Timelines** are the lines formed by a set of fluid particles that were marked at a previous instant in time, creating a line or a curve that is displaced in time as the particles move, see Fig. 1.5.

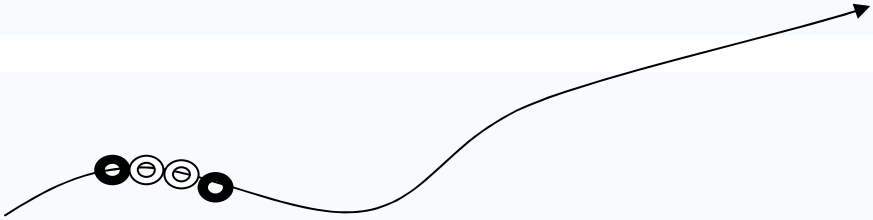

Fig. 1.5 Timeline

By definition, streamlines defined at a single instant in a flow do not intersect. This is so because a fluid particle cannot have two different velocities at the same point. Similarly streaklines cannot intersect themselves or other streaklines, because two particles cannot be present at the same location at the same instance of time. However, pathlines are allowed to intersect themselves or other pathlines (except the starting and end points of the different pathlines, which need to be distinct). In simple terms, streamlines and streaklines are like a snapshot of the flow field whereas pathlines are time-history of the flow.

In a steady flow, the streamline, pathline and streakline all coincide. In unsteady flow they can be different. Streamlines are easily generated mathematically while pathline and streaklines are obtained through experiments.

A region bounded by streamlines is called a **streamtube**. Because the streamlines are tangent to the flow velocity field, fluid that is inside a stream tube must remain forever

within that same streamtube. A scalar function whose contour lines define the streamlines is known as the **stream function**.

1.6 Application of Streamlines

Streamline can be quite useful in fluid dynamics. For example, Bernoulli's principle, which expresses conservation of mechanical energy, is only valid along a streamline. Also, the curvature of a streamline is an indication of the pressure change perpendicular to the streamline. The instantaneous centre of curvature of a streamline is in the direction of increasing pressure and the magnitude of the pressure gradient can be calculated from the curvature of the streamline.

1.7 Mass Conservative Streamline Tracking for a CFD Velocity Field

The accuracy of tracked streamlines for CFD velocity fields depends on the conservation of mass as indicated in [3, 4, 5, 6, 1, 7, 2, 13]. In computational mathematics, drawing a closed streamline is one of the measurements for the accuracy of numerical methods. Several authors [4, 7, 2] have shown that the streamlines tracked used mass conservative methods are more accurate than the other methods which do not conserve mass.

1.8 My Work (Simplification)

This thesis explains a simplified method of the procedure described by Li [6]. Chapter 4 explains all the steps involved and also shows two examples. The examples show the accuracy of the simplified method and the complications involved. The main advantage of the simplified method is that it saves valuable time.

Next chapter will explain what mass conservation is, the equations for streamlines and a brief introduction to mesh (or grid).

Chapter 2 Fundamentals

This chapter introduces the basic knowledge on mass conservation and the equation describing mass conservation, the equations for streamlines, and then mesh (or grid) for tracking streamlines for CFD velocity fields.

2.1 Mass Conservation

Conservation of mass simply means mass inflow equals mass outflow.

Let us consider a small volume of fluid V_0 fixed in space with a density ρ. Let dV be a small fluid element from within V_0 as shown in the following figure (Fig. 2.1).

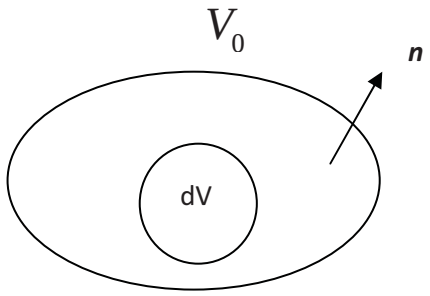

Fig. 2.1 Volume of fluid V_0 and dV

The mass, M, of this small fluid element dV is given by:

$$M = \rho dV \ .$$

So the total mass, M_0, over the volume, V_0, is given by

$$M_0 = \int_{V_0} \rho dV \ .$$

If the fluid has a velocity **v** and so the density ρ of the fluid varies with time *t,* the change in the total mass M_0 is given by

$$\frac{d}{dt}M_0 = \frac{\partial}{\partial t}\int_{V_0}\rho dV = \int_{V_0}\frac{\partial \rho}{\partial t}dV\,. \tag{2.1}$$

The last term is obtained by considering that the volume is fixed in space. So the total change in mass over time is given by:

$$\frac{d}{dt}M_0 = \int_{V_0}\frac{\partial \rho}{\partial t}dV\,. \tag{2.2}$$

Lets now consider the total outflow of the fluid mass.

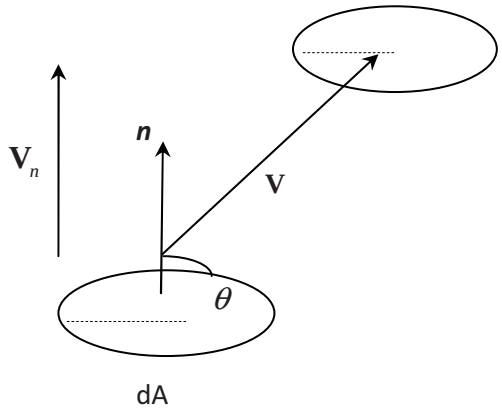

Fig. 2.2 Normal component $\mathbf{V}_n$ of velocity field **V**

Assume that the fluid is bounded by the surface A_0. The amount of mass flowing through the small portion (refer to Fig. 2.2), dA, of the total surface is given by:

$$\rho\,\mathbf{V}_n\,dA = \rho\,\mathbf{V}\cdot\mathbf{n}\,dA\,,$$

where $\mathbf{V}_n$ is the projection of the velocity field $\mathbf{V}$ on $\mathbf{n}$, and $\mathbf{n}$ is the unit normal.

So the total out-flow of the fluid mass over the surface A_0 per unit time is:

$$\oint_{A_0} \rho \mathbf{V}_n \, dA = \oint_{A_0} \rho \mathbf{V} \cdot \mathbf{n} \, dA = \oint_{A_0} \rho v_k n_k dA, \tag{2.3}$$

where $\mathbf{V} = (v_1, v_2, v_3)$ and $\mathbf{n} = (n_1, n_2, n_3)$. By applying divergence theorem, the integral is transformed into a volume integral as follows:

Replace the term $n_k dA$ in the surface integral with the volume element dV insert the differential operator $\frac{\partial}{\partial x_k}$ to act on the remaining portion of the integrand as shown:

$$\oint_{A_0} \rho v_k n_k dA = \int_{V_0} \frac{\partial}{\partial x_k} (\rho v_k) \, dV = \int_{V_0} div(\rho \mathbf{V}) \, dV, \tag{2.4}$$

where *div* is the divergence defined as $div = \frac{\partial}{\partial x_1} + \frac{\partial}{\partial x_2} + \frac{\partial}{\partial x_3}$.

Eq. (2.4) is equal to the negative of Eq. (2.2), hence:

$$\oint_{A_0} \rho v_k n_k dA = -\frac{d}{dt} M_0,$$

$$\int_{V_0} div(\rho \mathbf{V}) dV + \int_{V_0} \frac{\partial \rho}{\partial t} dV = 0,$$

$$\int_{V_0} \left[div(\rho \mathbf{V}) + \frac{\partial \rho}{\partial t} \right] dV = 0. \tag{2.5}$$

According to the mass conservation law, Eq. (2.5) must always hold, thus the integrand inside [ ] must vanish. The term inside [ ] can be further simplified as follows:

$$\frac{\partial \rho}{\partial t} + div(\rho \mathbf{V}) = 0 \,. \qquad (2.6)$$

This is called the *Continuity Equation.*

In the case of incompressible fluids, ρ is a constant, hence $\frac{\partial \rho}{\partial t} = 0$.

So the continuity equation reduces to $div\,\mathbf{V} = 0$.

2.2 Streamlines

Consider a flow at a certain time instant and draw velocity vectors at a large number of points distributed in the domain of flow. The collection of these vectors defines a vector field called the velocity field. Starting at a certain point in the flow, we may draw a line that is tangential to the velocity vector at each point. This generally curved three-dimensional line is called a streamline as shown in Fig. 2.3.

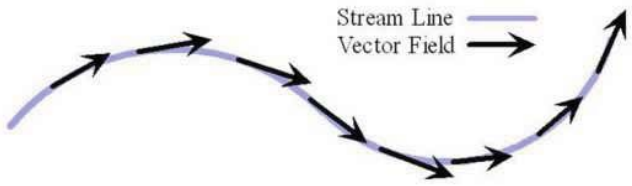

Fig. 2.3 Streamlines

A streamline is a line that is tangential to the direction of the vector field at every point along the line. For a velocity field $\mathbf{V} = \mathbf{V}(x, y, z, t) = u\,\mathbf{i} + v\,\mathbf{j} + w\,\mathbf{k}$ the equation of the streamline is

$\mathbf{V}\times dr = 0$ where dr = element of length along the streamline: $dr = \mathbf{i}\,dx + \mathbf{j}\,dy + \mathbf{k}\,dz$.

Since

$$\mathbf{V}\times dr = \begin{vmatrix} \mathbf{i} & \mathbf{j} & \mathbf{k} \\ u & v & w \\ dx & dy & dz \end{vmatrix},$$

thus

$$0 = \begin{vmatrix} v & w \\ dy & dz \end{vmatrix}\mathbf{i} - \begin{vmatrix} u & w \\ dx & dz \end{vmatrix}\mathbf{j} + \begin{vmatrix} u & v \\ dx & dy \end{vmatrix}\mathbf{k},$$
$$0 = \left[vdz - wdy\right]\mathbf{i} - \left[udz - wdx\right]\mathbf{j} + \left[udy - vdx\right]\mathbf{k}.$$

that is,

$$vdz - wdy = 0 \qquad udz - wdx = 0 \qquad udy - vdx = 0,$$

$$vdz = wdy \qquad udz = wdx \qquad udy = vdx,$$

$$\frac{dy}{v} = \frac{dz}{w} \qquad \frac{dx}{u} = \frac{dz}{w} \qquad \frac{dx}{u} = \frac{dy}{v},$$

$$\therefore \frac{dz}{w} = \frac{dy}{v} = \frac{dx}{u}.$$

Hence a streamline is the graph of the solution of $\frac{dz}{w} = \frac{dy}{v} = \frac{dx}{u}$ or written as vector form as $\frac{d\mathbf{X}}{dt} = \mathbf{V}$ (where $\mathbf{X} = (x, y, z)$).

In order to plot the streamline we choose a starting point, (x_0, y_0, z_0), and integrate $\frac{d\mathbf{X}}{dt} = \mathbf{V}$ from that point through the velocity field,

i.e. $$\int d\mathbf{x} = \int \mathbf{V} dt ,$$

$$(x, y, z) = \int \mathbf{V} dt .$$

We use CFD velocity fields obtained from the Navier-Stokes equations which govern fluid flows because it can be solved numerically for most of practical problems.

2.3 Mesh Construction

Since the velocity field calculated by computer is discrete, I only consider discrete velocity fields (CFD velocity fields) in this thesis. The calculations of CFD velocity fields normally are based a mesh (or grid). For three-dimensional problems, the commonly used CFD velocity fields are for hexahedral and tetrahedral meshes. In this thesis, I consider tetrahedral mesh only. A hexahedral mesh can be subdivided into tetrahedral mesh and then use the methods introduced in this thesis to track streamlines.

The CFD velocity fields at the vertices of hexahedrons are three dimensional vectors. The initial velocity field inside the tetrahedron is calculated using computers through linear interpolation. A hexahedron can be subdivided into either six or five tetrahedra. Fig. 2.4 shows the subdivision of a hexahedron into six tetrahedrons.

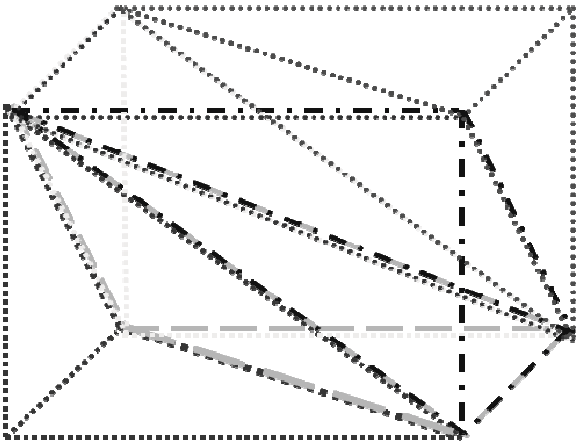

Fig. 2.4 subdivision of a hexahedron into six tetrahedra

Fig. 2.5 shows the subdivision of a tetrahedron into four smaller tetrahedra. The coordinates of the centre point O is taken as the average of the coordinates of four vertices of tetrahedron $ABCD$.

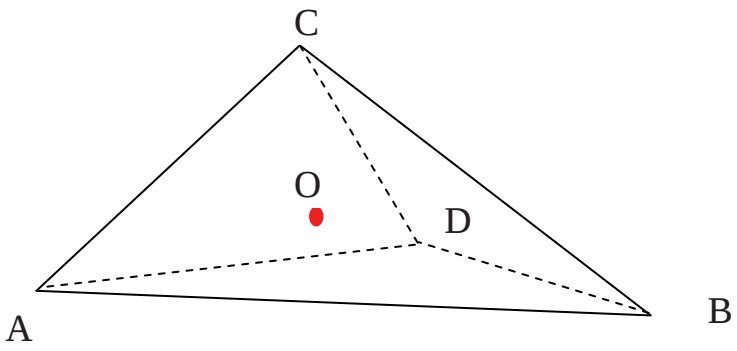

Fig. 2.5 Subdivision of a tetrahedron into four tetrahedra

Chapter 3 Review of Mass Conservative Streamline Tracking Methods

This chapter reviews the existing mass conservative streamline tracking methods for both two- and three- dimensional CFD velocity fields [4, 6]. For a given CFD velocity field, we start from the construction of mass conservative velocity field for quadrilateral and tetrahedral meshes. We then track streamlines for the constructed mass conservative velocity field using existing results.

3.1 Mass Conservative Streamline Tracking Method for 2D CFD Velocity Fields

The streamline for two-dimensional CFD velocity fields is generated from cell to cell for quadrilateral meshes. The streamline within each component in the subdivided cell is drawn by the exact expressions for tangent curves for two-dimensional linear vector fields given in [11]. We start from the linear interpolation of CFD velocity fields over a triangular domain, and end at the algorithm of streamline tracking.

3.1.1 Linear interpolation over a triangular domain

This subsection introduces how to obtain a velocity field over a triangular domain for a CFD velocity field. A quadrilateral is divided into two triangles by connecting two non neighboring vertexes. Then a linear velocity field $\mathbf{V}_l$ can be constructed over the triangular domain if the velocity field $\mathbf{V}$ at the three vertices of the triangle is given, i.e.

$$\mathbf{V}_l = \mathbf{A}\,\mathbf{X} + \mathbf{B}, \qquad (3.1)$$

where $\mathbf{A}=\begin{pmatrix} a_{11} & a_{12} \\ a_{21} & a_{22} \end{pmatrix}$ is a constant matrix, and $\mathbf{B}=\begin{pmatrix} b_1 \\ b_2 \end{pmatrix}$ is a vector matrix, $\mathbf{X}=\begin{pmatrix} x_1 \\ x_2 \end{pmatrix}$ is the coordinate vector.

The process of the construction is as follows.

- Substitute each of the coordinates of the three vertices and its corresponding velocity vector into Eq. (3.1) and get six linear equations.
- Solve the six equations for the six unknowns that are the elements in matrix **A** and vector **B**.

3.1.2 Construction of a mass conservative linear velocity fields over a quadrilateral

Mass conservation for an incompressible fluid means that

$$\nabla \cdot \mathbf{V} = 0 .$$

Substituting $\mathbf{V}_l$ into the above equation leads to

$$Trace(\mathbf{A}) = \nabla \cdot \mathbf{V}_l = 0 ,$$

i.e. linear velocity field $\mathbf{V}_l$ satisfies the law of mass conservation if and only if the trace of coefficient matrix **A** equals to zero.

The construction of a mass conservative linear interpolation for a given CFD velocity field on a quadrilateral is now described below. We take quadrilateral $ABCD$ in Fig. 3.1 as an example. Let O be an interior point of quadrilateral $ABCD$, often taken as the centre that calculated by averaging the horizontal and vertical coordinates of the four vertices for the horizontal and vertical coordinates respectively if the fourteen equations

described below in this paragraph are solvable and have an unique solution, otherwise chosen as a point close to the centre. Now we construct a mass conservative linear interpolation for the given CFD velocity field on quadrilateral $ABCO$. The CFD velocity field is given at the vertices of quadrilateral $ABCD$. We can construct a mass conservative linear interpolation as given by Eq. (3.1) on each of triangles ABO and BCO if we can assign appropriate vector to the linear velocity field at point O such that the trace of matrix A on each of the two triangles is zero. For each triangle, we have seven equations in which two for one of three vertices and one for mass conservation and eight unknowns in which six in Eq. (3.1) (four for matrix A and two for vector B) and two for the vector of velocity field at point O. Putting the two triangles together, we have fourteen equations and fourteen unknowns because the vector of velocity field at point O is the same for the two triangles. If such a linear system is not solvable, the point O must be on the straight line segment AC. For this case, choosing O close to the center guarantees the system is solvable and has a unique solution. Up to now, we have constructed a mass conservative linear interpolation over quadrilateral $ABCO$. Considering now the quadrilateral $ADCO$, the velocity field is known at the four vertices after adding the calculated velocity vector at O. Quadrilateral $ADCO$ can now be subdivided in the same manner as was the quadrilateral $ABCD$. Thus we can repeat the above procedure until the interpolation is obtained in any required part of the original quadrilateral. Although this has the potential to lead an infinite process, there is no need to construct the interpolation on the whole domain of quadrilateral $ABCD$ for tracking streamlines as shown in next subsection (Subsection 3.1.3).

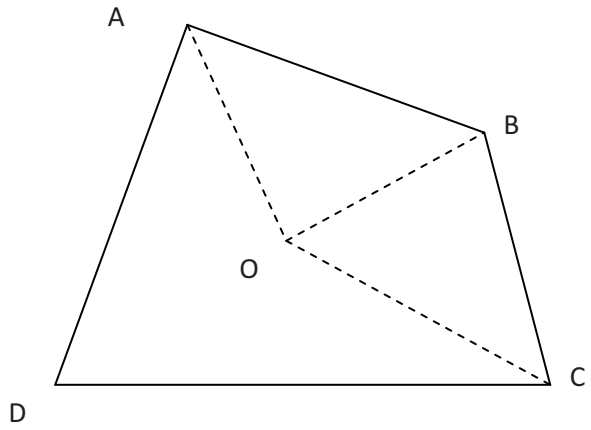

Fig. 3.1 Notation used to describe the construction of mass conservative interpolations for two triangles that from a sub-region of a quadrilateral

3.1.3 Streamlines for mass conservative linear velocity fields over a triangular domain

Nielson *et al* [11] derived exact expressions for two dimensional tangent curves within the context of piecewise linearly varying vector fields for all possible cases. These expressions are in terms of vector $\mathbf{B}$, matrix $\mathbf{A}$ as defined in Eq. (3.1) and the eigenvalues of $\mathbf{A}$. These expressions can be used for visualizing tangent curves for vector fields with linear interpolation of the data of the vector fields at the vertices in each triangle. The expressions in [11] can be used to draw streamline in each triangle. In this subsection we describe how to track a streamline in the whole domain of the velocity field. Since we draw streamline cell by cell, it is enough to show the streamline tracking method for a single cell.

Fig. 3.1 is used for the explanation for Step 1 and Fig. 3. 2 for the explanation for the other steps. The streamlines described in the following steps mean that they are drawn

using one of the expressions given in [11] according to the eigenvalue classification of matrix $\mathbf{A}$. The steps in the streamline tracking algorithm are as follows.

1. Find the quadrilateral that contains the seed point and divide the quadrilateral into two triangles such as ABC and ADC by connecting points A and C with a straight line segment. If the linear interpolations of the velocity field given in Eq. (3.1) on both triangles are mass conservative, draw the exact streamline segment that goes through the seed point in one triangle, e.g. ABC; Otherwise go to Step 2. If the intersection of the streamline segment with the boundary of the triangle ABC lies on AC, take the intersection as endpoint or seed point and draw the streamline segment in triangle ACD and return to Step 1; Otherwise take the intersection as seed point and go to Step 1 (for a new quadrilateral).

2. Assuming that the seed point is in quadrilateral $B_2B_3C_3C_2$ in Fig. 3.2, calculate the coordinates of the centre point O_1 of quadrilateral $B_2B_3C_3C_2$ and if the fourteen equations described in Subsection 3.1.2 are not solvable choose any point close to the center as O_1, and then go to step 3.

3. Construct mass conservative linear velocity field by the method given in Subsection 3.1.2 and draw streamline segment in quadrilateral $B_2B_3C_3C_2$ by the following process. Assuming that the seed point is in triangle $B_2B_3O_1$, we can construct a mass conservative linear velocity field by the method given in Subsection 3.1.2 in quadrilateral $B_2B_3O_1C_2$ and draw the streamline segment that going through the seed point in triangle $B_2B_3O_1$.

a. If the streamline crosses the boundary of triangle $B_2B_3O_1$ on segment B_2B_3, take the intersection as endpoint or seed point in quadrilateral $A_2A_3B_3B_2$ and go to Step 1.

b. If the streamline crosses the boundary of triangle $B_2B_3O_1$ on segment B_3O_1, take the intersection as endpoint or seed point in quadrilateral $B_3C_3C_2O_1$ and go to Step 1. In this case, since $B_3C_3C_2O_1$ is still a quadrilateral so we can continue tracking streamline from step 1 again. O_2 in Fig. 2 is the O_1 in the next step when $B_3C_3C_2O_1$ cannot be divided into two triangles on which the linear interpolation of the velocity field given by Eq. (3.1) is not mass conservative for at least one of the triangles.

c. If the streamline crosses the boundary of triangle $B_2B_3O_1$ on segment B_2O_1, take the intersection as endpoint or seed point in triangle $B_2O_1C_2$ and draw streamline segment that going through the seed point.

   i. If the streamline crosses the boundary of triangle $B_2O_1C_2$ on segment B_2C_2, take the intersection as endpoint or seed point in quadrilateral $B_1B_2C_2C_1$ and go to Step 1.

   ii. If the streamline crosses the boundary of triangle $B_2O_1C_2$ on segment C_2O_1, take the intersection as endpoint or seed point in quadrilateral $B_3C_3C_2O_1$ and go to Step 1.

iii. If the streamline crosses the boundary of triangle $B_2O_1C_2$ on segment B_2O_1, take the intersection as seed point in triangle $B_2B_3O_1$, draw streamline using the linear velocity field that drew the streamline segment in $B_2B_3O_1$ in Step 3 and then go to one of Sub-steps a, b and c according to the intersection of the streamline with the boundary.

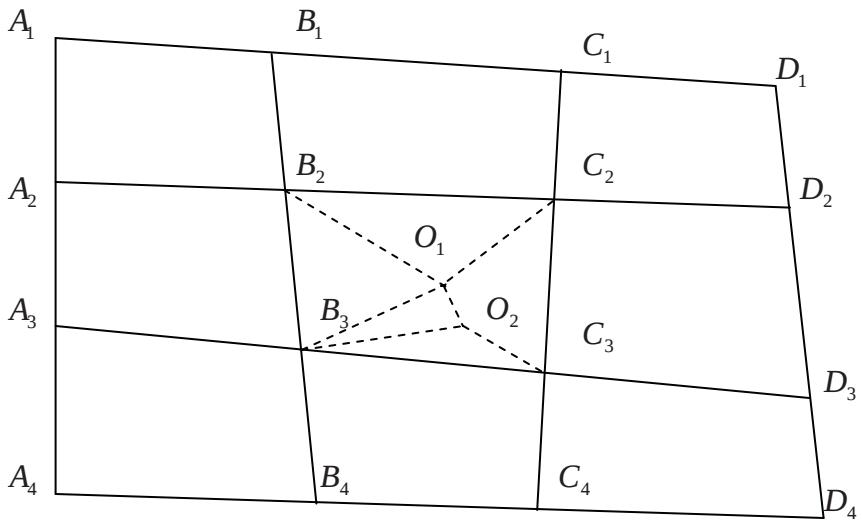

Fig. 3.2 Tracking streamline explanation

Streamlines can be drawn following the algorithm above. Examples in [4] shows that the streamlines tracked by the algorithm are much more accurate than the other existing methods.

3.2 A Mass Conservative Streamline Tracking Method for 3D CFD Velocity Fields

The streamline generation for three-dimensional CFD velocity fields is similar to that for two-dimensional CFD velocity fields introduced in Section 3.1. The streamline generation for this case is carried from cell to cell for tetrahedral meshes. The

streamline within each component in the subdivided cell is drawn by the exact expressions for tangent curves for two-dimensional linear vector fields given in [10]. A hexahedral mesh can be divided into tetrahedral mesh by dividing a tetrahedron into six tetrahedra as shown in Fig. 2.3.

3.2.1 Linear interpolation over a tetrahedral domain

This subsection gives a brief introduction on how to create a velocity field over a tetrahedral domain from the vectors of a given CFD velocity field at the vertices of the tetrahedron. We use linear interpolation here for the velocity field creation. The linear interpolation over a tetrahedral domain is similar to the interpolation over a triangular domain.

A linear velocity field $\mathbf{V}_l$ can be constructed over the tetrahedral domain if the vectors of velocity field $\mathbf{V}$ at the four vertices of the tetrahedron are given, i.e.

$$\mathbf{V}_l = \mathbf{AX} + \mathbf{B}, \qquad (3.2)$$

where $\mathbf{A} = \begin{pmatrix} a_{11} & a_{12} & a_{13} \\ a_{21} & a_{22} & a_{23} \\ a_{31} & a_{32} & a_{33} \end{pmatrix}$ is a constant matrix, and $\mathbf{B} = \begin{pmatrix} b_{11} \\ b_{21} \\ b_{31} \end{pmatrix}$ is a vector matrix.

$\mathbf{X} = \begin{pmatrix} x_{11} \\ x_{21} \\ x_{31} \end{pmatrix}$ is the coordinate vector.

The process of the construction is as follows.

- Substitute the coordinates of each of the four vertices of a tetrahedron and its corresponding velocity vector into Eq. (3.2) and get 12 linear equations.
- Solve the 12 equations for the 12 unknowns that are the elements in matrix $\mathbf{A}$ and vector $\mathbf{B}$.

The linear velocity field $\mathbf{V}_l$ is defined over the tetrahedron if the coordinate vector $\mathbf{X}$ varies over it and $\mathbf{V}_l = \mathbf{V}$ at all four vertices of the tetrahedron.

3.2.2 Construction of a mass conservative linear velocity fields over a tetrahedral domain

The equation of mass conservation for a three-dimensional incompressible fluid again is

$$\nabla \cdot \mathbf{V} = 0 .$$

Substituting $\mathbf{V}_l$ into the above equation leads to

$$Trace(\mathbf{A}) = \nabla \cdot \mathbf{V}_l = 0 ,$$

i.e. linear velocity field $\mathbf{V}_l$ satisfies the law of mass conservation if and only if the trace of coefficient matrix **A** equals to zero.

Now we introduce the construction of a linear mass conservative interpolation for a given CFD velocity field over a tetrahedral domain. We take tetrahedron $ABCD$ in Fig. 3.3 as an example. Let O be an interior point of tetrahedron $ABCD$, often taken as the centre that calculated by averaging the three coordinates of the four vertices' respectively if the fourteen equations described below in this paragraph are solvable and have a unique solution, otherwise chosen as a point close to the centre. How close

we choose a point O to the centre depends on the computer capacity available and the requirement of the accuracy. Now we construct a linear mass conservative interpolation for the given CFD velocity field over tetrahedrons $ABCO$, $ACDO$, and $ABDO$. The CFD velocity field is given at the vertices of tetrahedron $ABCD$. We can construct a linear mass conservative interpolation as given by Eq. (3.2) over each of tetrahedrons $ABCO$, $ACDO$, and $ABDO$ if we can assign appropriate vector to the linear velocity field at point O such that the trace of matrix $\mathbf{A}$ over each of the three tetrahedrons is zero. For each tetrahedron, we have thirteen equations in which three for one of four vertices and one for the law of mass conservation and fifteen unknowns in which twelve in Eq. (3.2) (nine for matrix $\mathbf{A}$ and three for vector $\mathbf{B}$) and three for the value of velocity field at point O. Putting the three tetrahedrons together, we have thirty-nine equations and thirty-nine unknowns because the value of velocity field at point O is the same for the three tetrahedrons. If such a linear system is not solvable, the point O must be in the triangle BCD. For this case, choosing O close to the centre guarantees the system is solvable and has a unique solution. Up to now, we have constructed a linear mass conservative interpolation over tetrahedrons $ABCO$, $ACDO$, and $ABDO$. Considering the tetrahedron $OBCD$, the velocity field is known at the four vertices after adding the calculated value of velocity field at O. The tetrahedron $OBCD$ can now be subdivided in the same manner as was the tetrahedron $ABCD$. Thus we can repeat the above procedure until the interpolation is obtained in any required part of the original tetrahedron $ABCD$. Although this has the potential to lead an infinite process, there is no need to construct the interpolation on the whole domain of tetrahedron $ABCD$ for tracking streamlines.

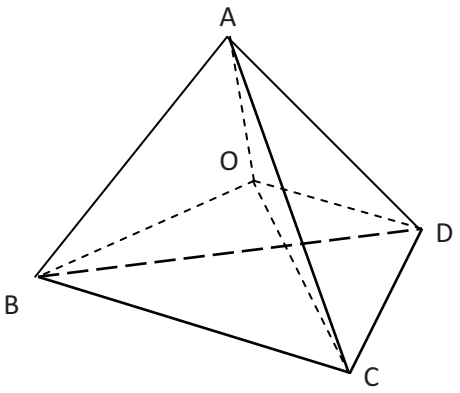

Fig. 3.3 A subdivision of a tetrahedron into four tetrahedrons

3.2.3 Mass Conservative Streamline Tracking Algorithm

In this subsection we describe how to track a streamline in the whole domain of a three-dimensional CFD velocity field. Since we draw streamline tetrahedron by tetrahedron, it is enough to describe the streamline tracking method for a single tetrahedron.

Fig. 3.4 is used for the explanation for the steps except for step 1. The streamline segments described in the following steps mean that they are drawn using one of the expressions given in [12] according to the eigenvalue classification of matrix **A**. The steps are as follows.

1. Find the tetrahedron that contains the seed. If the linear interpolation of the velocity field given in Eq. 3.2 over the tetrahedron is mass conservative, draw the exact streamline segment that goes through the seed point; Otherwise go to Step 2. Take the intersection of the streamline segment with the boundary of the tetrahedron as endpoint or seed point and go to Step 1 (for a new tetrahedron).

2. Assuming that the seed point is in tetrahedron $ABCD$ in Fig. 3.2, calculate the coordinates of the center point O of tetrahedron $ABCD$ and if the thirty nine equations described in last section are not solvable choose any point close to the center o, and then go to step 3.
3. Construct linear mass conservative vector field by the method given in last section and draw streamline segment in tetrahedron $ABCD$ by the following process. Assuming that the seed point is in tetrahedron $ACDO$, we can construct a linear mass conservative vector field by the method given in last section in tetrahedra $ABCO$, $ABDO$ and $ACDO$ and draw the streamline segment that going through the seed point in tetrahedron $ACDO$.
   a. If the streamline segment crosses the boundary of tetrahedron $ACDO$ on face ACD, take the intersection as endpoint or seed point in tetrahedron $ACDD_1$ and go to Step 1.
   b. If the streamline segment crosses the boundary of tetrahedron $ACDO$ on face OCD, take the intersection as endpoint or seed point in tetrahedron $OBCD$ and go to Step 1. In this case, since $OBCD$ is still a tetrahedron so we can continue tracking streamline from step 1 again.
   c. If the streamline segment crosses the boundary of tetrahedron $ACDO$ on faces ACO or ADO, take the intersection as endpoint or seed point in tetrahedra $ABCO$ or $ABDO$ respectively and draw streamline segment that going through the seed point. We take $ABCO$ as an example for the explanation of the procedures followed.

i. If the streamline segment crosses the boundary of tetrahedron $ABCO$ on face ABC, take the intersection as endpoint or seed point in tetrahedron AB_1BC and go to Step 1.

ii. If the streamline segment crosses the boundary of tetrahedron $ABCO$ on face OBC, take the intersection as endpoint or seed point in tetrahedron $OBCD$ and go to Step 1.

iii. If the streamline segment crosses the boundary of tetrahedron $ABCO$ on faces ABO or ACO, take the intersection as seed point in tetrahedra $ABDO$ or $ACDO$ respectively, draw streamline segment using the linear velocity field generated in Step 3 and then go to one of Sub-steps a, b and c according to the intersection of the streamline segment with the boundary.

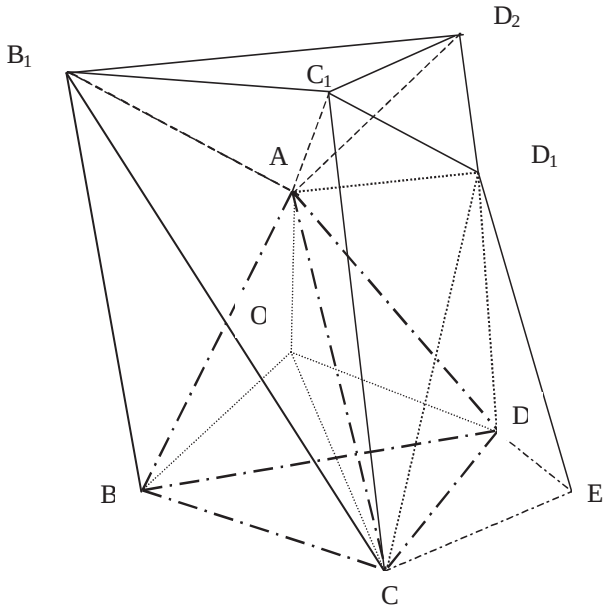

Fig. 3. 4 Streamline tracking explanation

3.2.4 Summary

Examples in [6] shows that the mass conservative streamlines are much more accurate than the streamlines tracked by other methods. However, the streamline tracking process may take time in subdividing tetrahedra into smaller tetrahedra to achieve mass conservative streamlines.

The following chapter describes how to simplify the process of the above streamline tracking for three-dimensional CFD velocity fields. The resulting method takes much less CPU time in tracking the same streamlines.

Chapter 4 Simplification Process

This chapter presents how to simplify the streamline tracking process introduced in last chapter for three-dimensional CFD velocity fields. The accuracy of the simplified method has been shown through two examples for analytical velocity fields. The reasons why we use analytical velocity fields include that we are able to compare the exact streamlines generated by the analytical fields with the tracked streamlines. The simplified method takes the same time as the non mass conservative streamline tracking method [12] in the tetrahedra where $f\mathbf{v}_l$ (f is a scalar function) satisfies the law of mass conservation and needs more time than the non mass conservative method in the tetrahedra where $f\mathbf{v}_l$ does not satisfy the law of mass conservation. It takes less time than the method given in [6]. The results in this chapter have been published in [12].

4.1 Streamline Tracking Algorithm

This section presents every step in the simplified algorithm for tracking streamlines. The flow chart of the algorithm is shown in Fig. 4.1. The algorithm has been coded in Matlab for the examples in next section.

Step 1: Locating the tetrahedron that contains the seedpoint

The streamline generation is carried out from cell to cell for tetrahedral meshes.

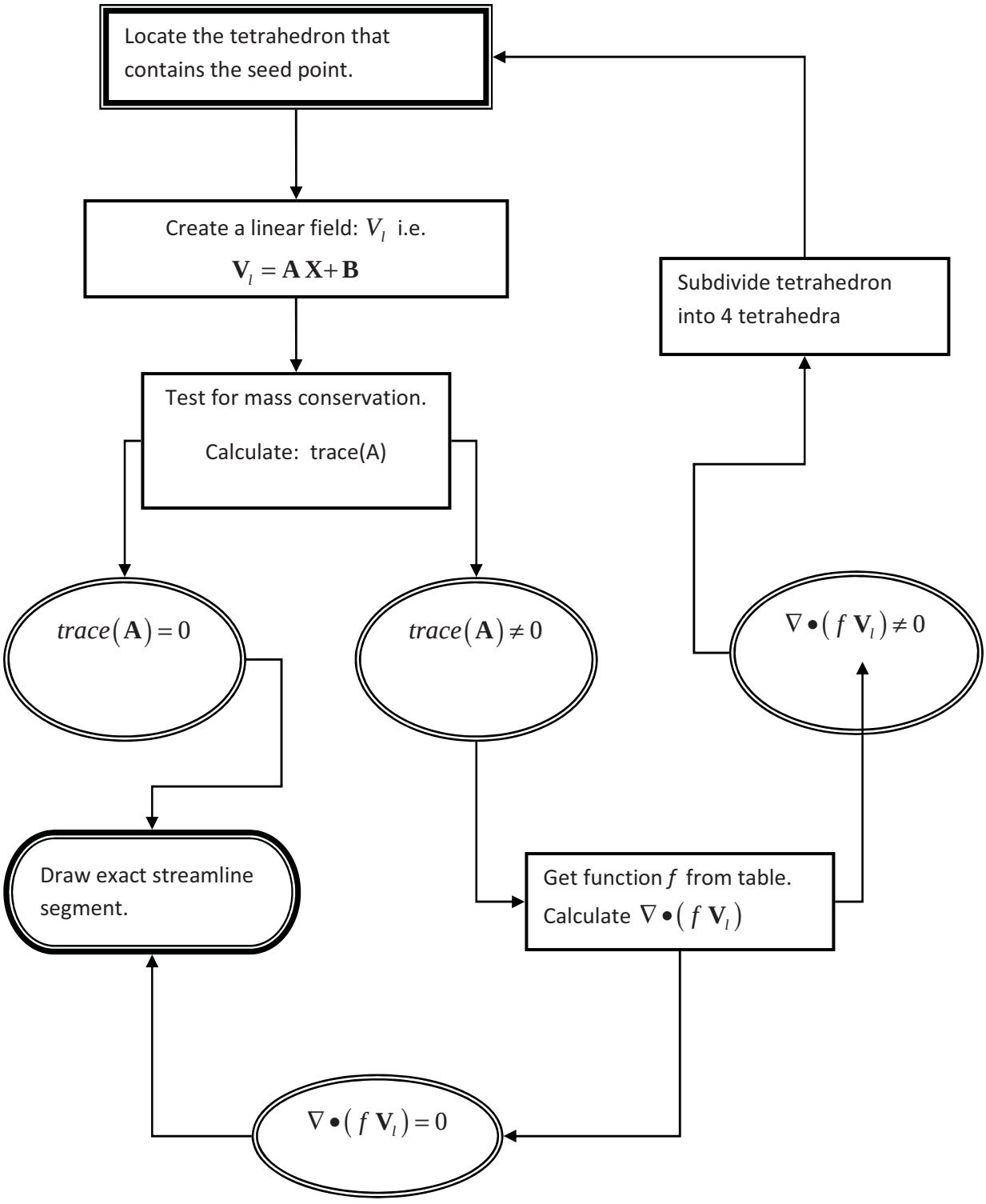

Fig. 4. 1 Flow chart of simplified streamline tracking method

Now consider a tetrahedron shown in Fig. 4.2. We use $X_1, X_2, X_3, \text{and } X_4$ to represent the vertices of the tetrahedron and also their coordinates. The procedure for the verification is as follows:

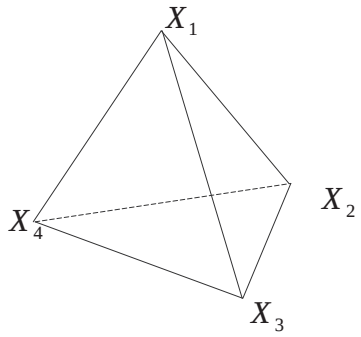

Fig. 4.2 A tetrahedron

Given a seedpoint P_0. We also use P_0 to represent its coordinates. Let

$$K_1 = \frac{\det\begin{bmatrix}\mathbf{P}_0-\mathbf{X}_2 & \mathbf{P}_0-\mathbf{X}_3 & \mathbf{P}_0-\mathbf{X}_4\end{bmatrix}}{\det\begin{bmatrix}\mathbf{X}_1-\mathbf{X}_2 & \mathbf{X}_1-\mathbf{X}_3 & \mathbf{X}_1-\mathbf{X}_4\end{bmatrix}},$$

$$K_2 = \frac{\det\begin{bmatrix}\mathbf{P}_0-\mathbf{X}_1 & \mathbf{P}_0-\mathbf{X}_3 & \mathbf{P}_0-\mathbf{X}_4\end{bmatrix}}{\det\begin{bmatrix}\mathbf{X}_2-\mathbf{X}_1 & \mathbf{X}_2-\mathbf{X}_3 & \mathbf{X}_2-\mathbf{X}_4\end{bmatrix}},$$

$$K_3 = \frac{\det\begin{bmatrix}\mathbf{P}_0-\mathbf{X}_1 & \mathbf{P}_0-\mathbf{X}_2 & \mathbf{P}_0-\mathbf{X}_4\end{bmatrix}}{\det\begin{bmatrix}\mathbf{X}_3-\mathbf{X}_1 & \mathbf{X}_3-\mathbf{X}_2 & \mathbf{X}_3-\mathbf{X}_4\end{bmatrix}},$$

$$K_4 = \frac{\det\begin{bmatrix}\mathbf{P}_0-\mathbf{X}_1 & \mathbf{P}_0-\mathbf{X}_2 & \mathbf{P}_0-\mathbf{X}_3\end{bmatrix}}{\det\begin{bmatrix}\mathbf{X}_4-\mathbf{X}_1 & \mathbf{X}_4-\mathbf{X}_2 & \mathbf{X}_4-\mathbf{X}_3\end{bmatrix}}.$$

The seedpoint P_0 is in the tetrahedron if $K_1 \geq 0, K_2 \geq 0, K_3 \geq 0, K_4 \geq 0$.

Step 2: Creating a linear mass conservative field

The vectors at the vertices of the tetrahedron are used to construct a linear velocity field inside the tetrahedron. The construction is as follows:

- The velocity field is a function of spatial variables i.e. $\mathbf{V}_l = \mathbf{V}(x, y, z)$

$$\mathbf{V}_l = \mathbf{AX} + \mathbf{B}, \qquad (4.1)$$

where $\mathbf{A} = \begin{pmatrix} a_{11} & a_{12} & a_{13} \\ a_{21} & a_{22} & a_{23} \\ a_{31} & a_{32} & a_{33} \end{pmatrix}$, $\mathbf{B} = \begin{pmatrix} b_{11} \\ b_{21} \\ b_{31} \end{pmatrix}$ and $\mathbf{X} = (x, y, z)^T$ is the co-ordinate vector.

- Let the coordinates of the four vertices be:

$$\mathbf{X}_1 = (x_1, y_1, z_1)$$
$$\mathbf{X}_2 = (x_1, y_2, z_2)$$
$$\mathbf{X}_3 = (x_3, y_3, z_3)$$
$$\mathbf{X}_4 = (x_4, y_4, z_4)$$

and the vectors at the four vertices be:

$$\mathbf{V}_1 = \mathbf{V}(x_1, y_1, z_1) = (v_{x_1}, v_{y_1}, v_{z_1})$$
$$\mathbf{V}_2 = \mathbf{V}(x_2, y_2, z_2) = (v_{x_2}, v_{y_2}, v_{z_2})$$
$$\mathbf{V}_3 = \mathbf{V}(x_3, y_3, z_3) = (v_{x_3}, v_{y_3}, v_{z_3})$$
$$\mathbf{V}_4 = \mathbf{V}(x_4, y_4, z_4) = (v_{x_4}, v_{y_4}, v_{z_4})$$

Substitute each of the coordinate vectors and its corresponding velocity vector into Eq. (4.1) and get twelve linear equations.

$$\left.\begin{aligned} v_{x_1} &= a_{11}x_1 + a_{12}y_1 + a_{13}z_1 + b_1 \\ v_{y_1} &= a_{21}x_1 + a_{22}y_1 + a_{23}z_1 + b_2 \\ v_{z_1} &= a_{31}x_1 + a_{32}y_1 + a_{33}z_1 + b_3 \end{aligned}\right\} \text{ at vertex } \mathbf{X}_1$$

$$\left.\begin{aligned} v_{x_2} &= a_{11}x_2 + a_{12}y_2 + a_{13}z_2 + b_1 \\ v_{y_2} &= a_{21}x_2 + a_{22}y_2 + a_{23}z_2 + b_2 \\ v_{z_2} &= a_{31}x_2 + a_{32}y_2 + a_{33}z_2 + b_3 \end{aligned}\right\} \text{at vertex } \mathbf{X}_2$$

$$\left.\begin{aligned} v_{x_3} &= a_{11}x_3 + a_{12}y_3 + a_{13}z_3 + b_1 \\ v_{y_3} &= a_{21}x_3 + a_{22}y_3 + a_{23}z_3 + b_2 \\ v_{z_3} &= a_{31}x_3 + a_{32}y_3 + a_{33}z_3 + b_3 \end{aligned}\right\} \text{at vertex } \mathbf{X}_3$$

$$\left.\begin{aligned} v_{x_4} &= a_{11}x_4 + a_{12}y_4 + a_{13}z_4 + b_1 \\ v_{y_4} &= a_{21}x_4 + a_{22}y_4 + a_{23}z_4 + b_2 \\ v_{z_4} &= a_{31}x_4 + a_{32}y_4 + a_{33}z_4 + b_3 \end{aligned}\right\} \text{at point } O$$

Solve above twelve equations for the twelve unknowns that are the elements in matrix $\mathbf{A}$ and vector $\mathbf{B}$ and calculate $trace(\mathbf{A})$.

Step 3: Test for mass conservation and draw streamline

If $trace(\mathbf{A}) = 0$, the exact streamline is plotted according to the eigenvalues of $\mathbf{A}$ using the formulae given in the table 1 in Appendix 1.

If $trace(\mathbf{A}) \neq 0$, a function f can be found from table 2 in Appendix 1 according to the eigenvalues of A and then compute $\nabla \cdot (f\,\mathbf{V}_l)$.

1. $\nabla \cdot (f\,\mathbf{V}_l) = 0$.

The exact streamline is plotted according to the eigenvalues of $\mathbf{A}$ using the formulae given in the table 1 in Appendix 1.

2. $\nabla \cdot (f \mathbf{V}_l) \neq 0$.

Subdivide the tetrahedral into four tetrahedra and go to Step 1.

Next section will show some examples follow the procedure in this section.

4.2 Examples

Two examples are presented in this section. The comparisons between tracked and exact streamlines are shown in the same figure as well as their projections on different two-dimensional planes.

Example 1

Given the velocity field $\mathbf{V} = \left(xz - y, yz + x, -z^2 \right)$ within the domain $[-2,2] \times [-2,-2] \times [0,1]$ in the Cartesian coordinate system (x, y, z). The seedpoint is chosen to be [0.08340862239242, 0.11420596179972, 1].

The streamlines of the velocity field in this example approach z plane asymptotically. The efficiency of the streamline tracking method will be seen from the behaviors of tracked streamlines close to z plane.

Cell size (hexahedron): 2 × 2× 0.5

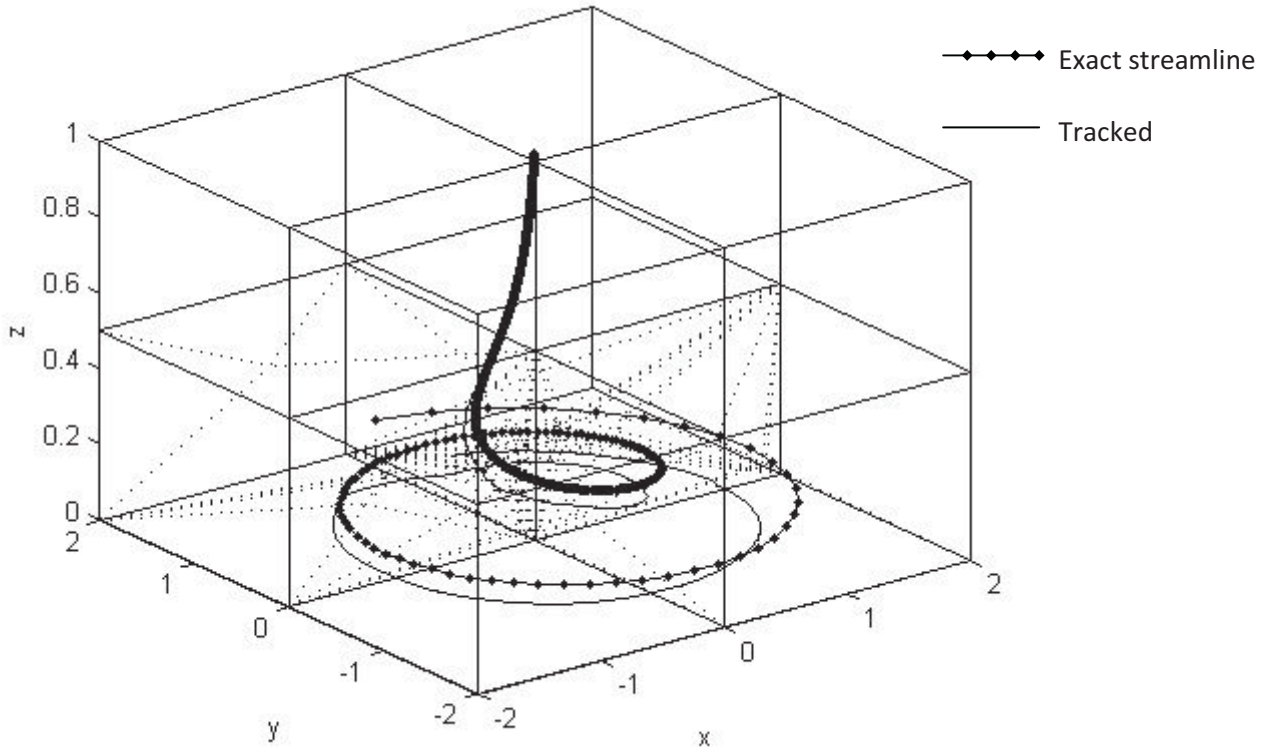

Fig. 4.2 Three Dimensional view of the streamlines

The streamline starts at the top and spirals downwards. The total number of hexahedra used in this process was 9 and the total number of tetrahedra used was 48.

For simplicity I have omitted to show the hexahedron subdividing into tetrahedra however all subdivisions of tetrahedra are shown by the dot lines.

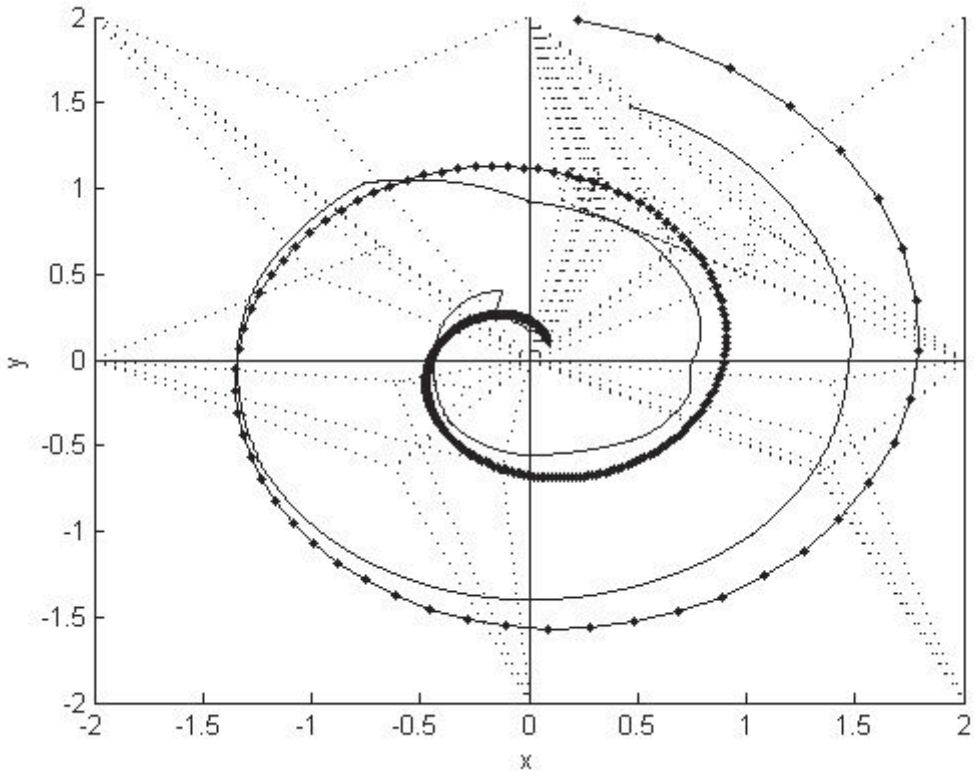

Fig. 4.3 Birds eye (*x*, *y*) view of the streamlines

The above plot shows that although there were about 40 tetrahedra subdivided the tracked streamline still differs from the exact at a lot of locations. The tracked streamline is not as smooth as the exact initially although it smooth out toward the end.

Another observation is that the tracked streamline seems to spiral does not outward faster than the exact streamline towards the end.

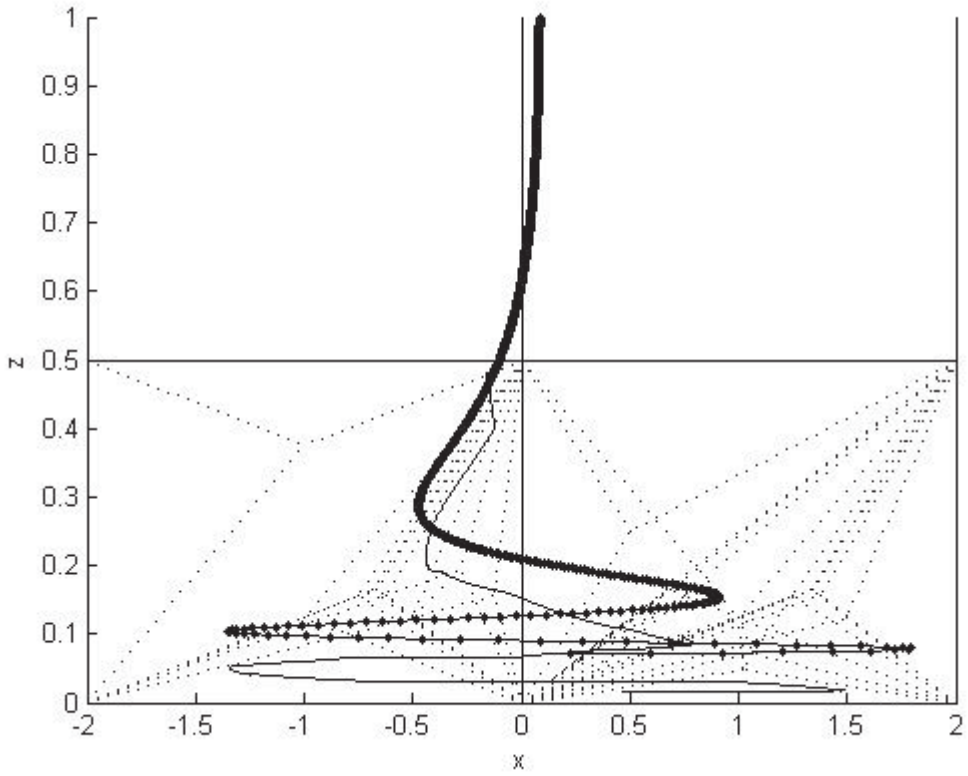

Fig. 4.4 (*x*, *z*) view of the streamlines

As noted earlier the tracked streamline is not as smooth as the exact and it is quite apparent in Fig. 4.4.

It is also noted that the bottom z plane incurs a lot of tetrahedron subdivisions than the top.

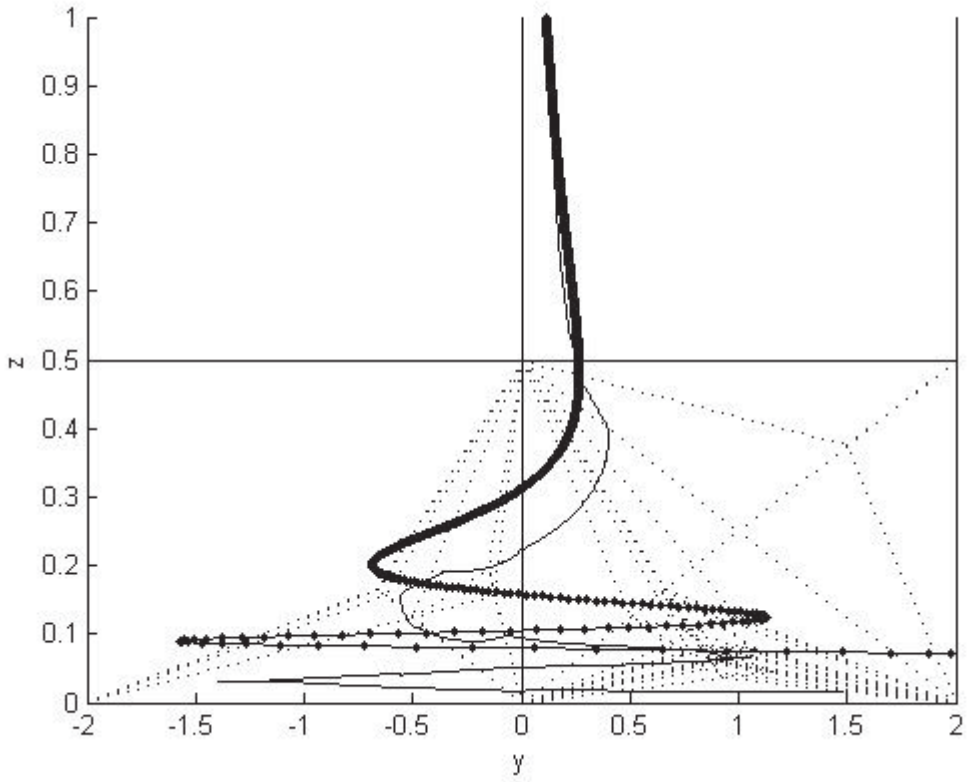

Fig. 4.5 (y, z) view of the streamlines

Fig. 4.5 also shows that as the streamline nears the bottom, the margin for errors increases.

Now I shall reduce the size of the x and y components of the hexahedron and observe the results.

Cell size (hexahedron): 1 × 1 × 0.5

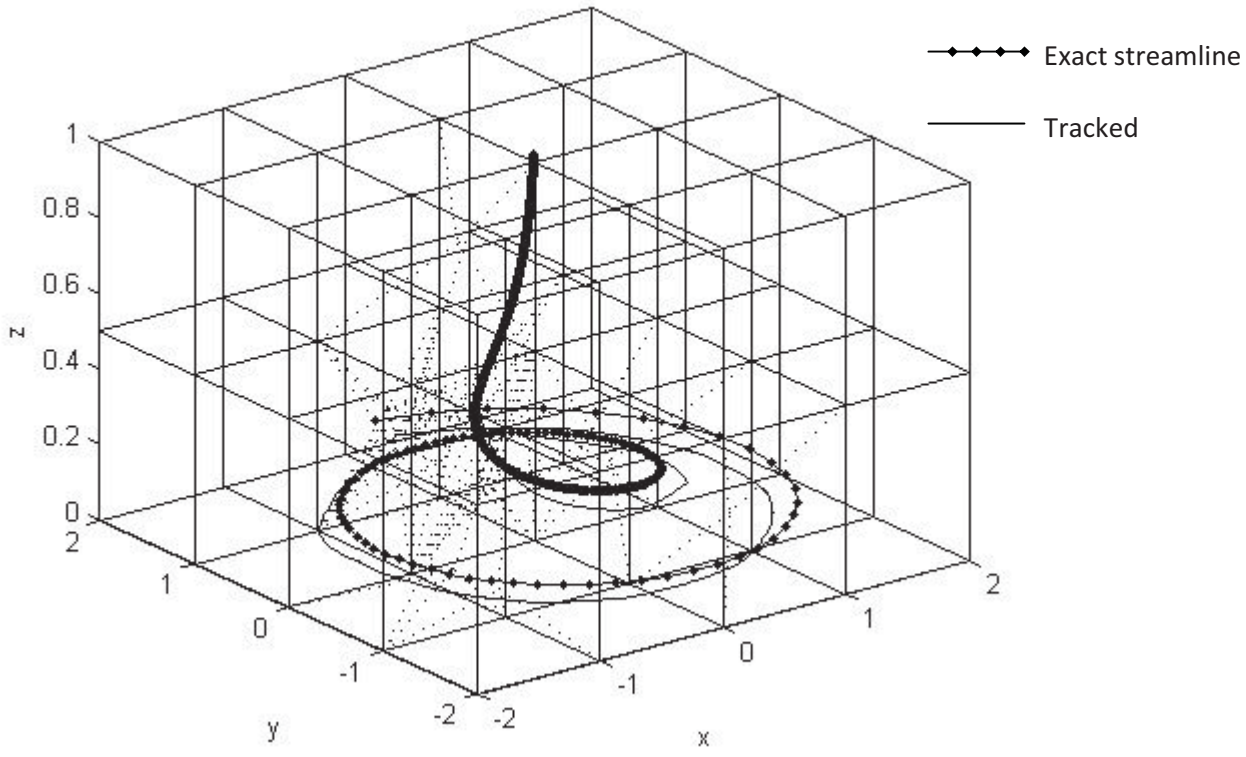

Fig. 4.6 Three Dimensional view of the streamlines

19 hexahedra and 98 tetrahedra were used to achieve this streamline. As it is shown there were more tetrahedra subdivisions than the previous case.

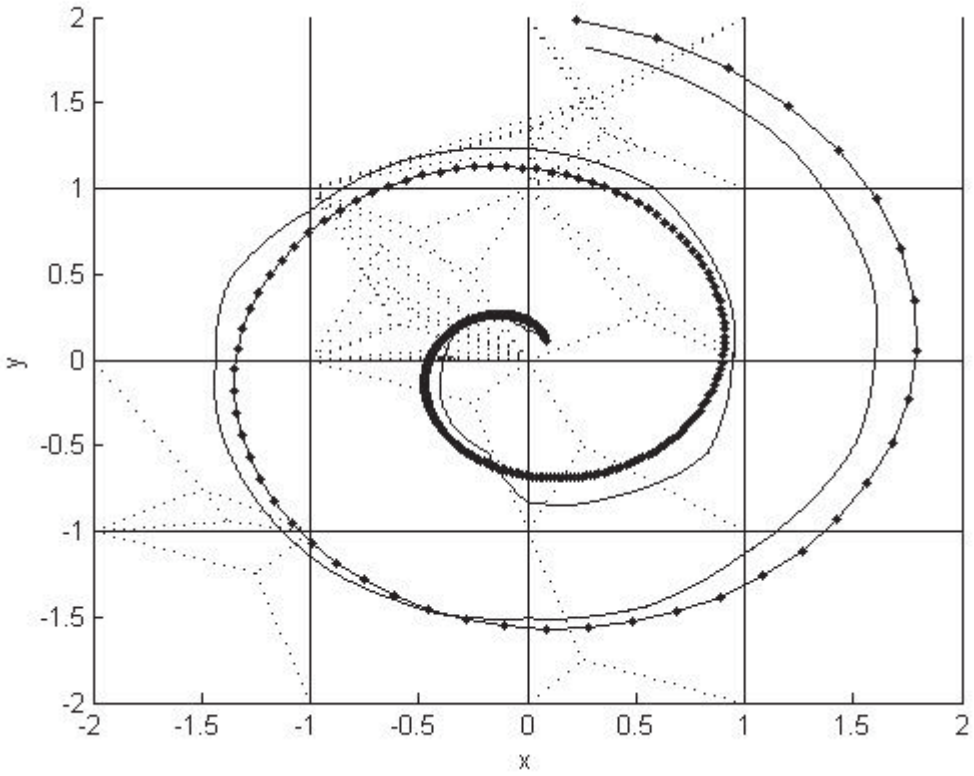

Fig. 4.7 (*x*, *y*) view of the streamlines

In comparison to the previous case, this tracked streamline is much more accurate.

The tracked streamline is not as smooth as the exact streamline at the beginning, both streamlines run almost parallel towards the end.

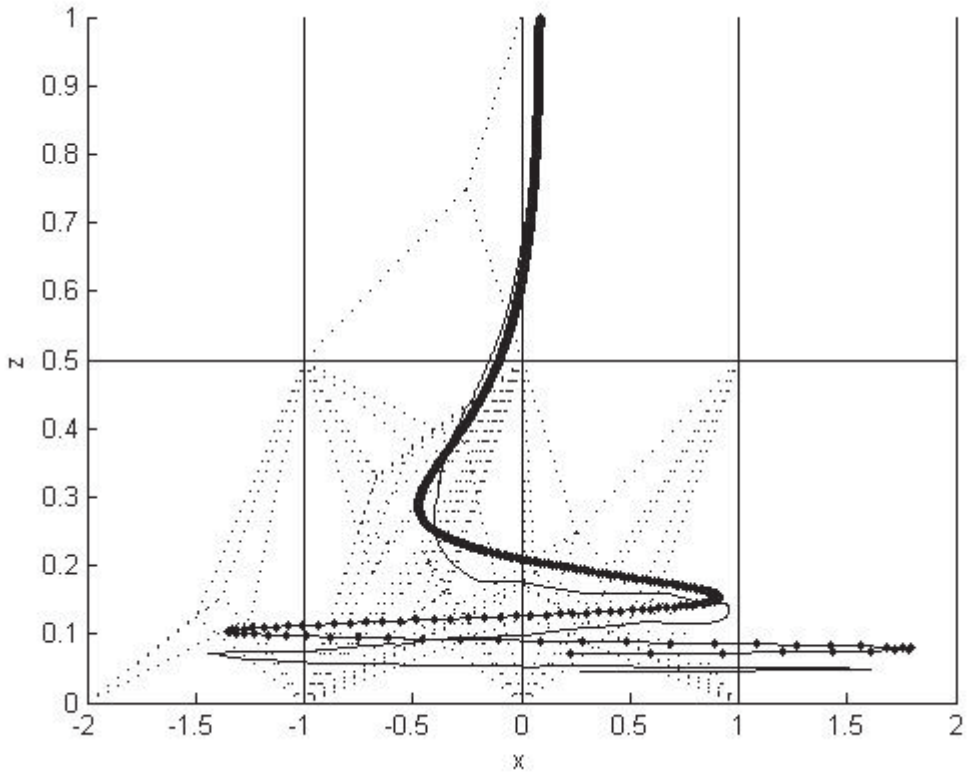

Fig. 4.8 (*x*, *z*) view of the streamlines

There has been tetrahedron subdivision at the top as well as the bottom z plane. There is not much change from Fig. 4.4. The margin of errors increases as the streamline approaches *z* plane.

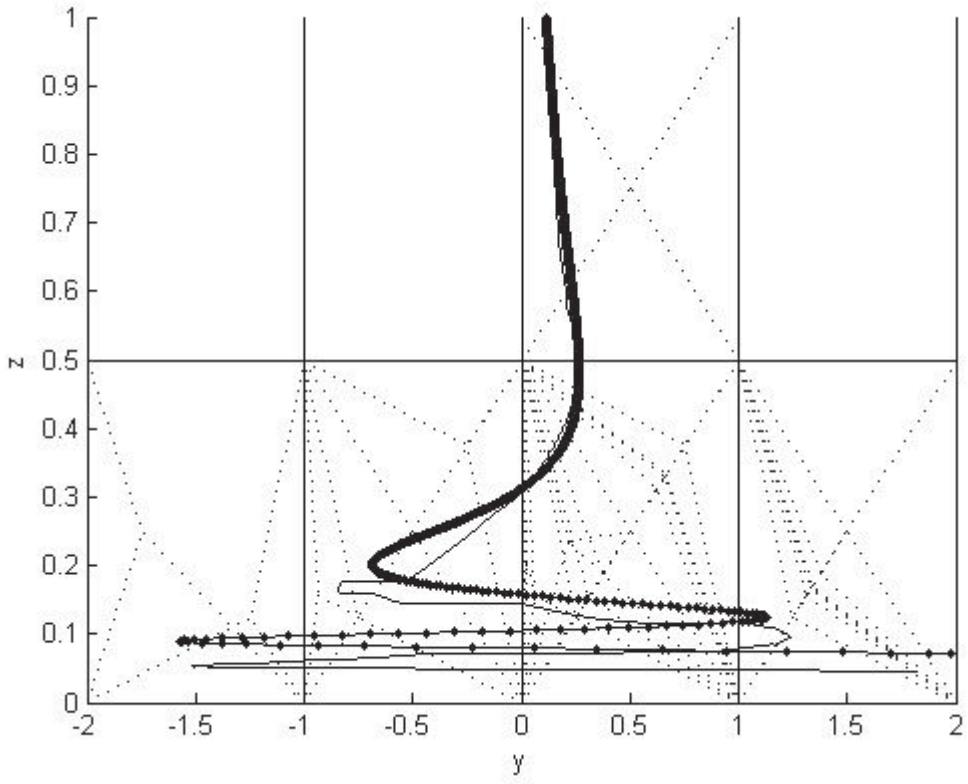

Fig. 4.9 (*y*, *z*) view of the streamlines

Again we notice that as the tracked streamline spirals toward *z* plane, the marigin of errors is increasing.

Since I reduced the sizes of x and y components of the previous hexahedron and I noticed a remarkable reduction in errors especially in the Fig. 4.6. However I am not completely satisfied with the result. I believe if I reduced the x and y component again I would achieve a better result.

So I would now proceed with my cell size reduction and observe the results.

Cell size (hexahedron): 0.5 × 0.5 × 0.5

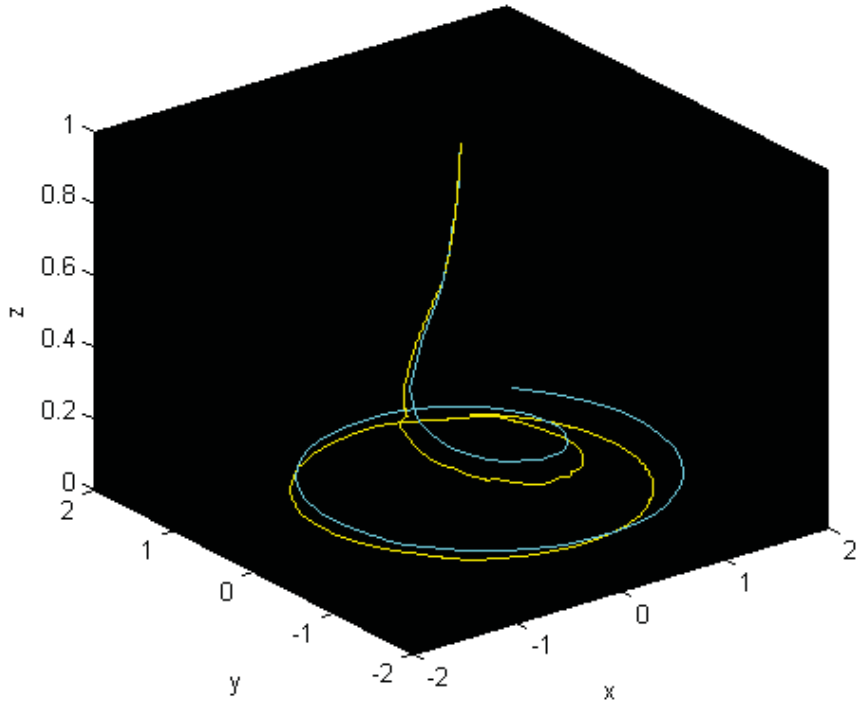

Fig. 4.10 Three Dimensional view of the streamlines

I used 34 hexahedrons and 178 tetrahedrons to achieve this plot.

I was still dissatisfied with the nature of the tracked streamline in the block with vertices

(-1, -0.5), (-1, 0), (-0.5, -0.5), (-0.5, 0).

In the other parts of the plot, there was not much difference in comparison to the previous plot.

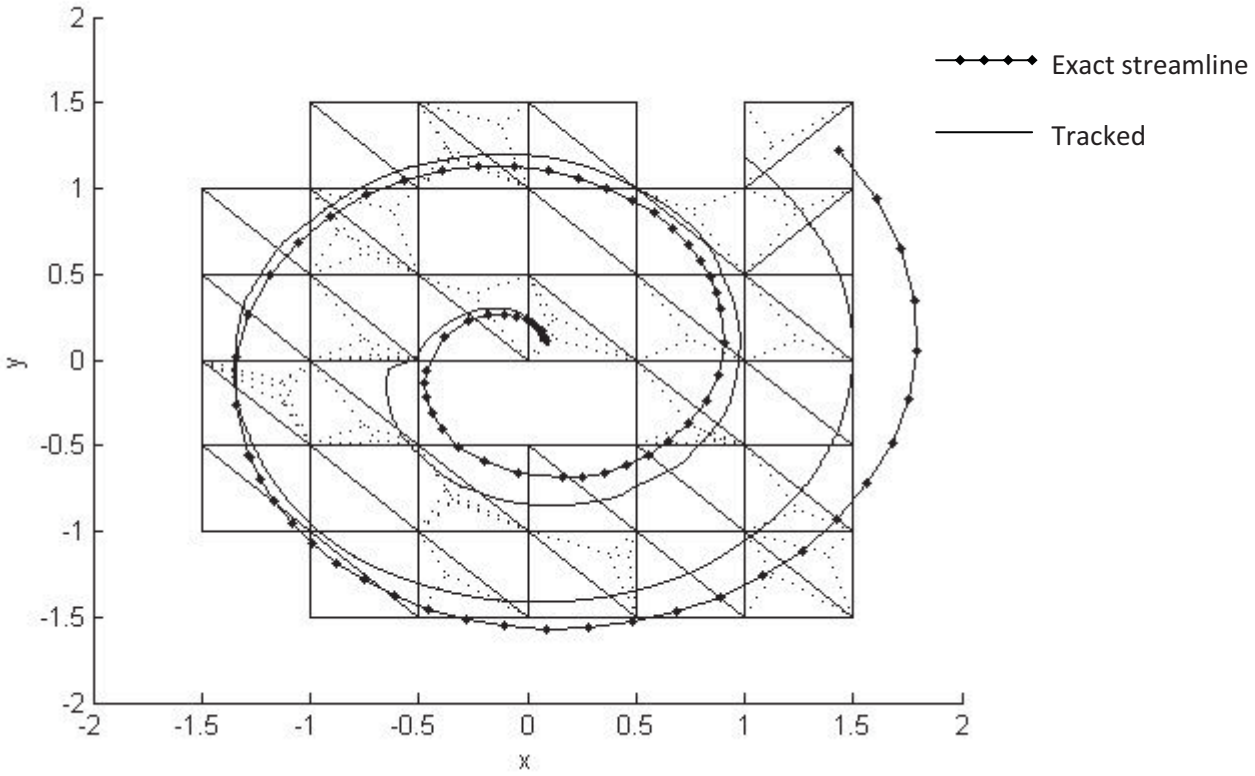

Fig. 4.11 (*x*, *y*) view of the streamlines

There was not much difference between this plot and Fig 4.7. The accuracy of the tracked streamline suffers as it nears to z plane.

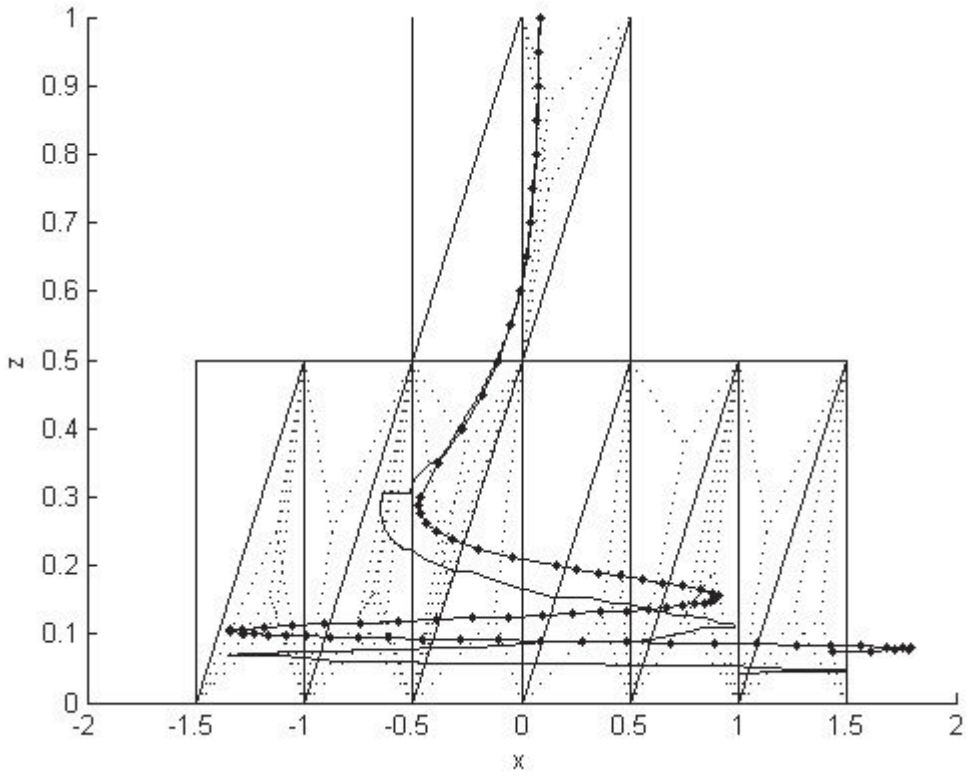

Fig. 4.12 (*x*, *z*) view of the streamlines

There was not much difference between this plot and Fig 4.8. The diference between the tracked and exact streamlines can be seen clearly in Fig. 4.12.

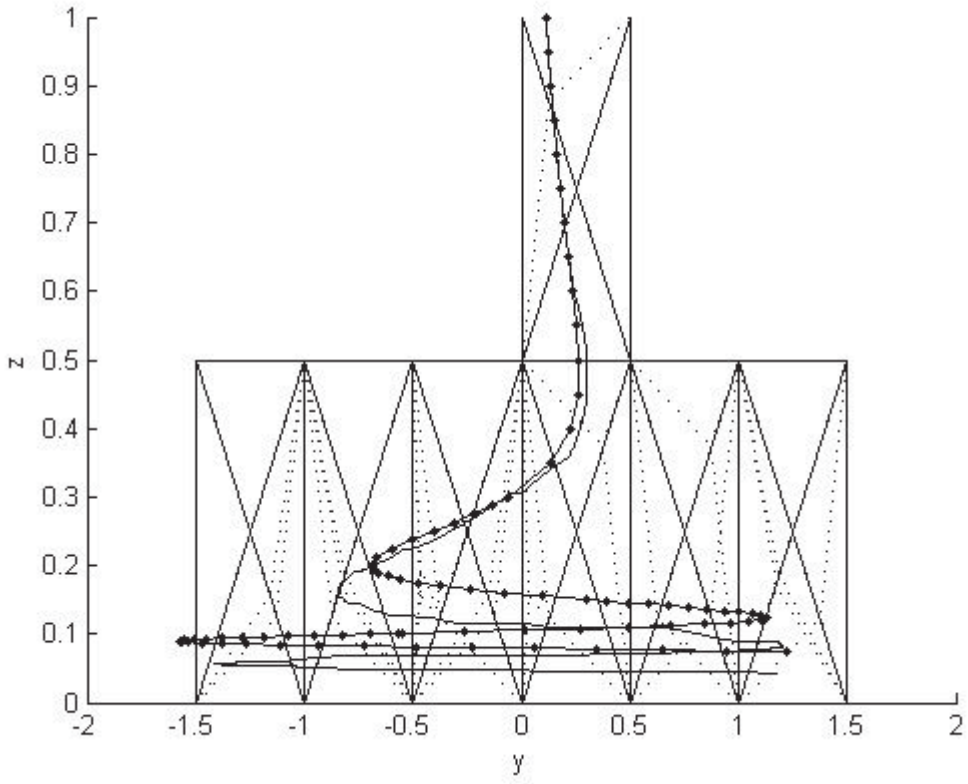

Fig. 4.13 (*y*, *z*) view of the streamlines

Again I notice that there is not much difference between this plot and Fig. 4.9.

Also note that every cell has tetrahedron subdivisions. And yet the margin of errors increases as the plot approaches z plane.

Since there has not been much change in the accuracy of the plot after reducing the x and y component for the second time, I have decided to reduce z component and observe the results.

Cell size (hexahedron): 0.5 × 0.5 × 0.25

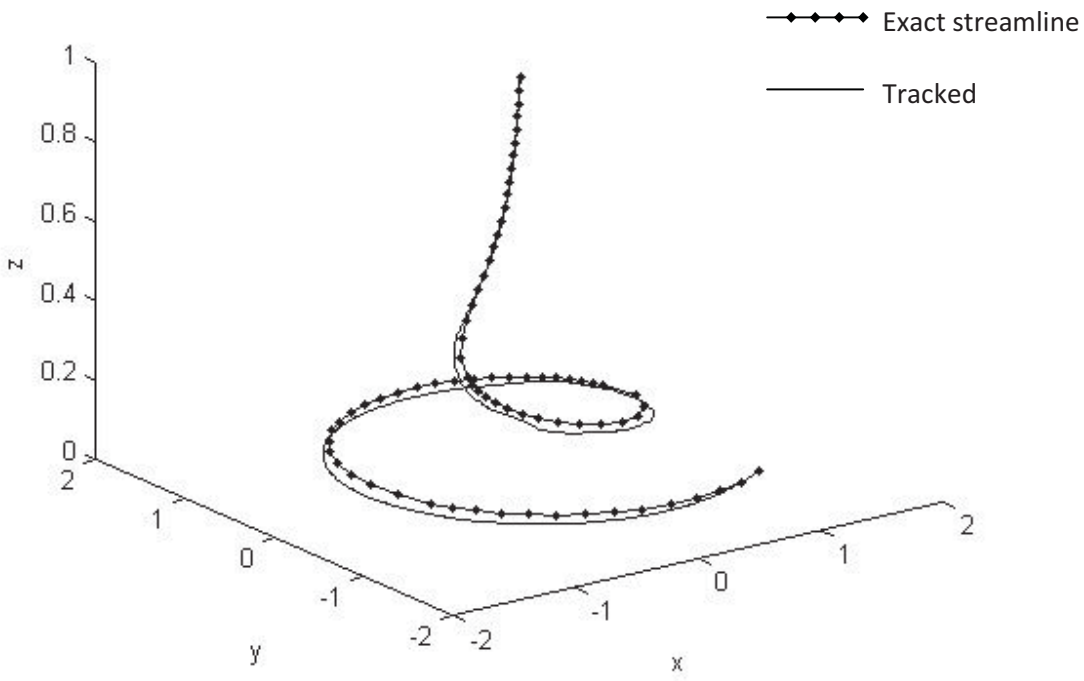

Fig. 4.14 Three Dimensional view of the streamlines

A total of 146 hexahedrons and 85 tetrahedrons were used in the plotting of this streamline.

In this view it is quite clear that a high level of accuracy has been achieved.

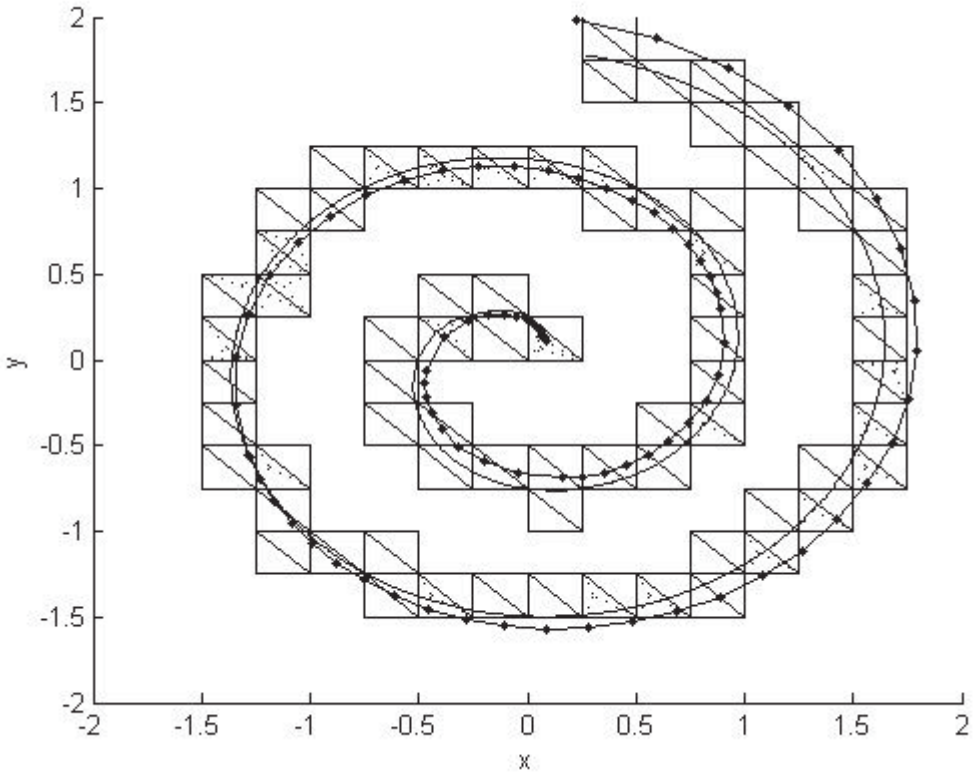

Fig. 4.15 (x, y) view of the streamlines

The tracked and exact streamlines run almost parallel, but the tracked streamline spirals outwards slightly slower than the exact streamline. Compared to previous plots the streamline is much smoother in nature in all the cells.

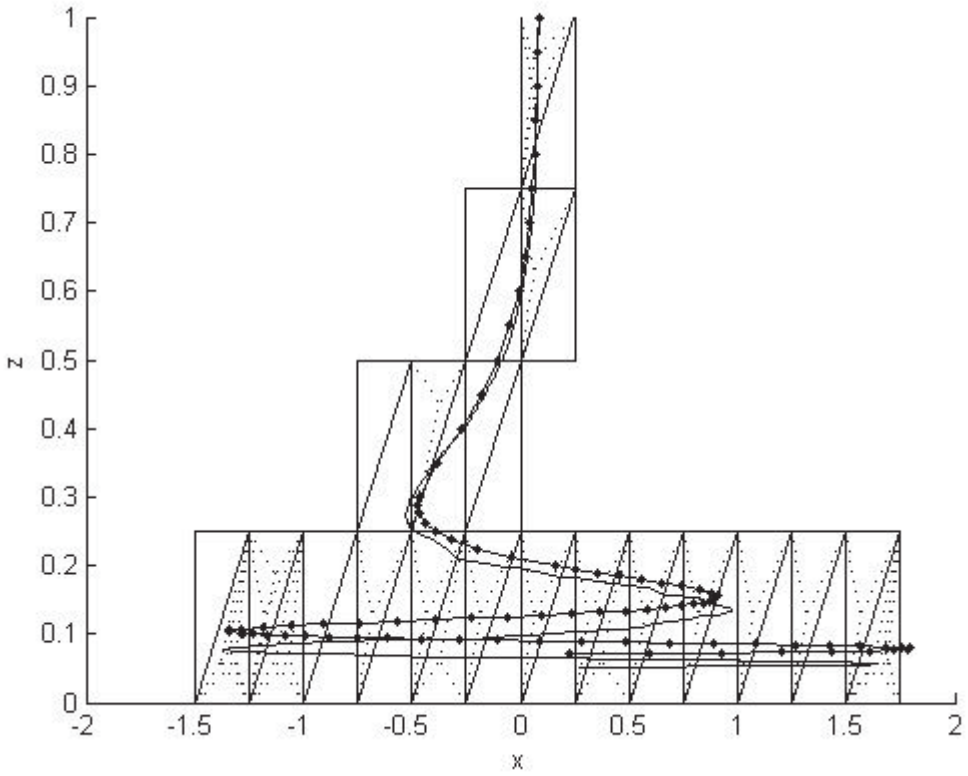

Fig. 4.16 (x, z) view of the asymptotic streamlines

The tracked and exact streamlines descend almost together but separate towards z plane. This shows that the decision to reduce the size of the z component was appropriate.

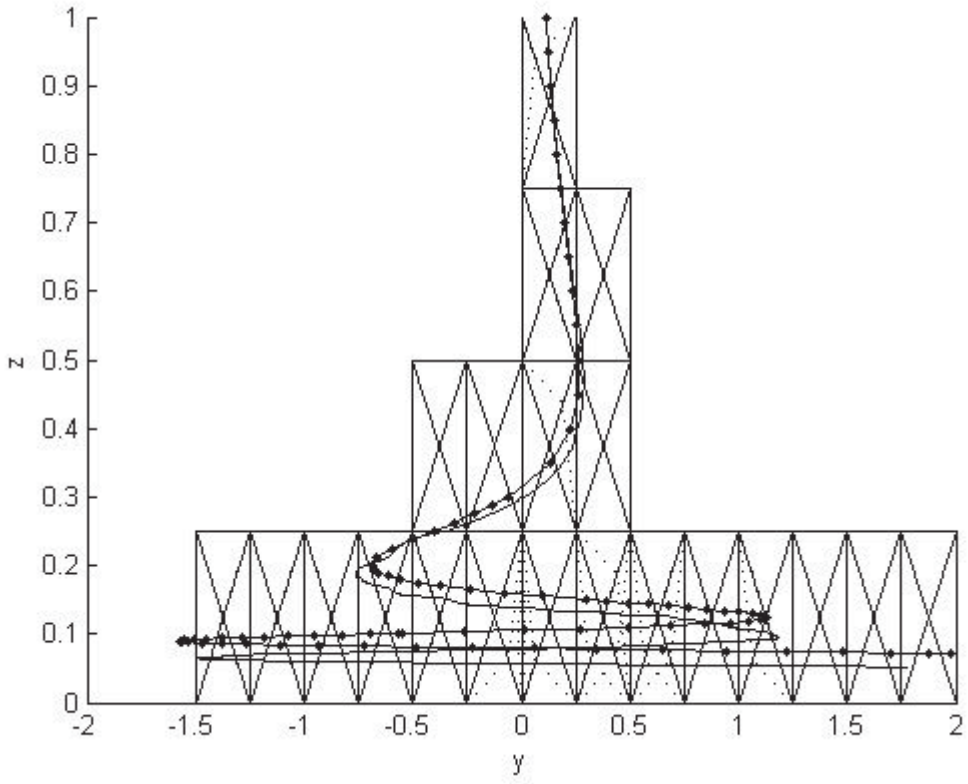

Fig. 4.17 (y,z) view of the streamlines

Here it is observed that both the streamlines descend almost together but separate towards the end. However they both run parallel to each other.

So I have come to the conclusion that if the cell size is further reduced, the accuracy of the streamline will be improved, so much so that perhaps at some stage the tracked streamline will match the exact streamline. The streamline tracking method introduced in this thesis can be applied to CFD velocity fields obtained by measurement using devices. It is important to set the mesh nodes before measurement such that more nodes should be put the possible complex regions for accurate results.

Example 2

Velocity Field

$$\mathbf{V}=\left(\frac{2x(z-1)}{x^2+y^2}-\frac{0.4y}{\sqrt{x^2+y^2}},\frac{2y(z-1)}{x^2+y^2}+\frac{0.4x}{\sqrt{x^2+y^2}},\frac{-2\left(\sqrt{x^2+y^2}-9\right)}{\sqrt{x^2+y^2}}\right)$$

In domain: $[-10,10]\times[-10,10]\times[0,2]$ in Cartesian coordinate system (x,y,z). The seed point is $[5.9996,6.2867,1.3924]$.

The streamlines of this velocity field are closed. The accuracy of the streamline tracking method can be seen from the differences of tracked streamlines at the initial and terminal points.

Size of hexahedron: 1 × 1 × 0.5

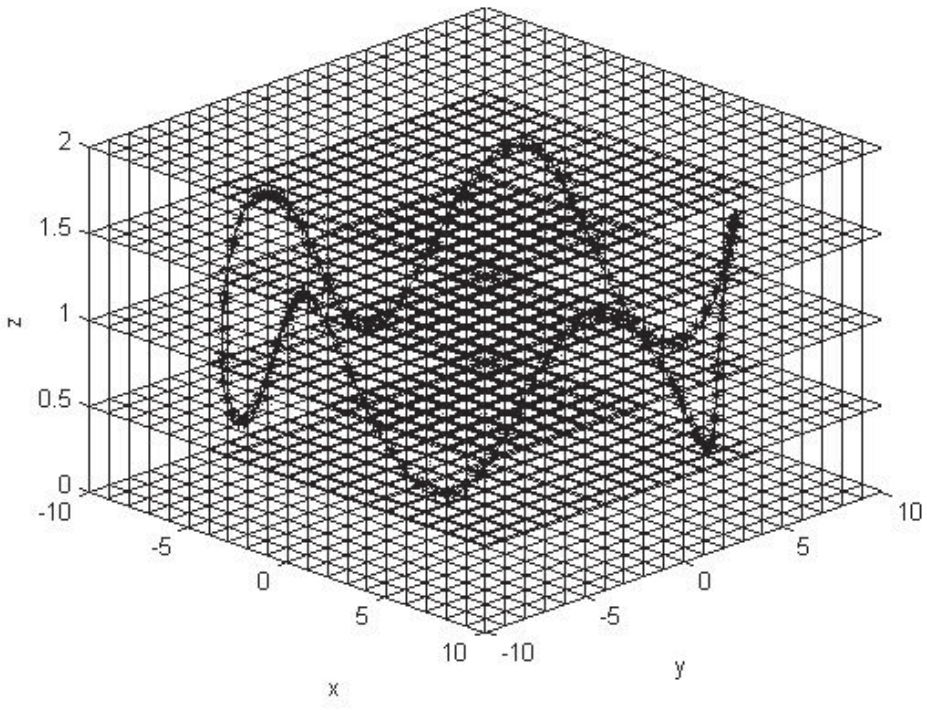

Fig. 4.18 A three dimensional view of the torus with the mesh

The torus is a closed streamline, oscillating between the 5 z-planes as shown in Fig. 4.18. The stars, (*) represent the exact streamline and the line (-), represents the streamline plotted using simplified algorithm. A total of 104 hexahedra and 525 tetrahedra were used in this process.

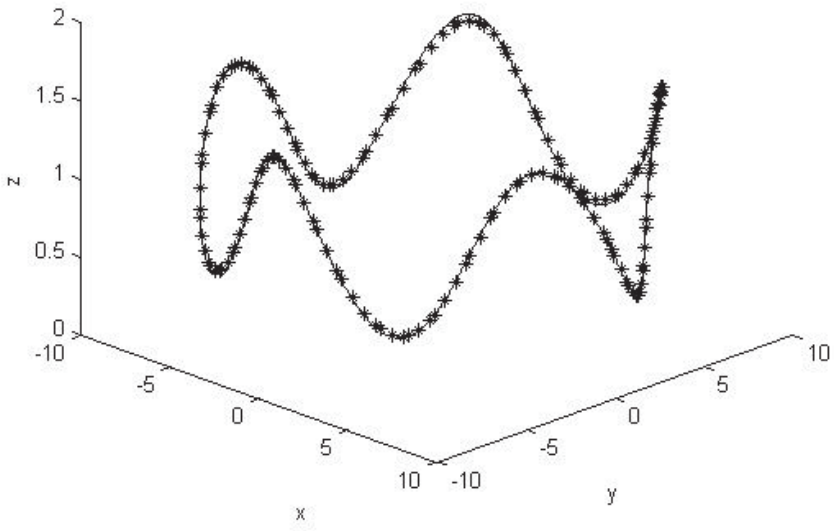

Fig. 4.19 A three dimensional view of the torus without the mesh

The tracked and exact streamlines coincide at so many points it seems that they are almost the same. The margin for errors is very low.

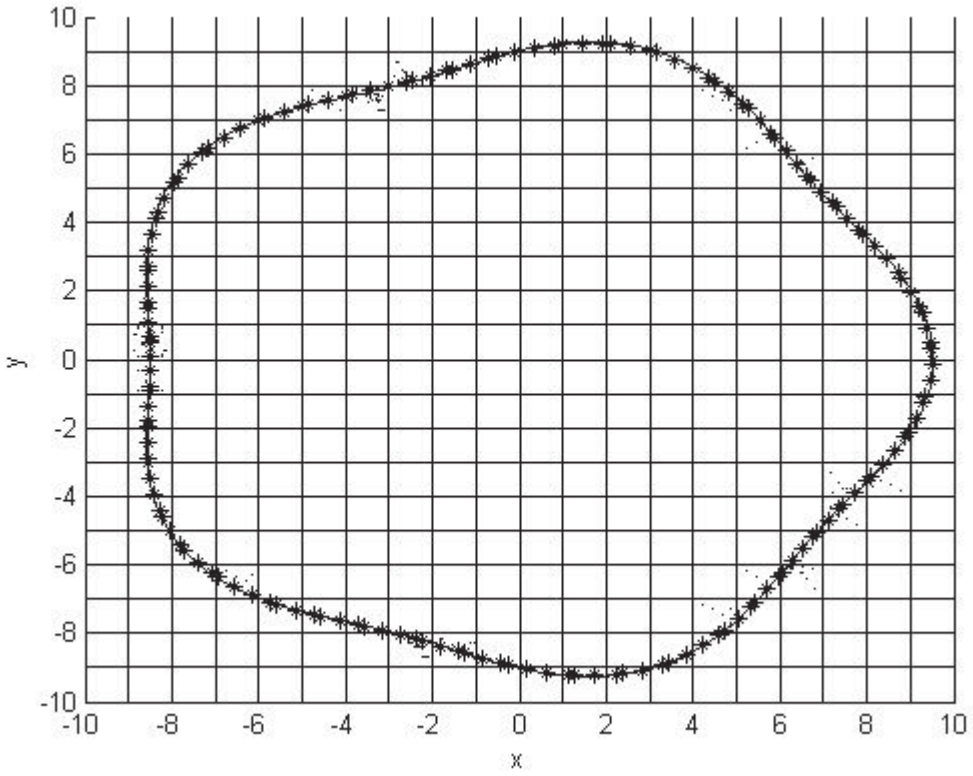

Fig. 4.20 The birds eye (*x*, *y*) view of the torus

In Fig. 4.20, we can see the subdivisions of the tetrahedra. As many as 58 tetrahedra were subdivided in this plot. As it was intended the subdivisions were conducted to uphold the law of mass conservation and from the above plot it is apparent that the subdivisions were highly accurate.

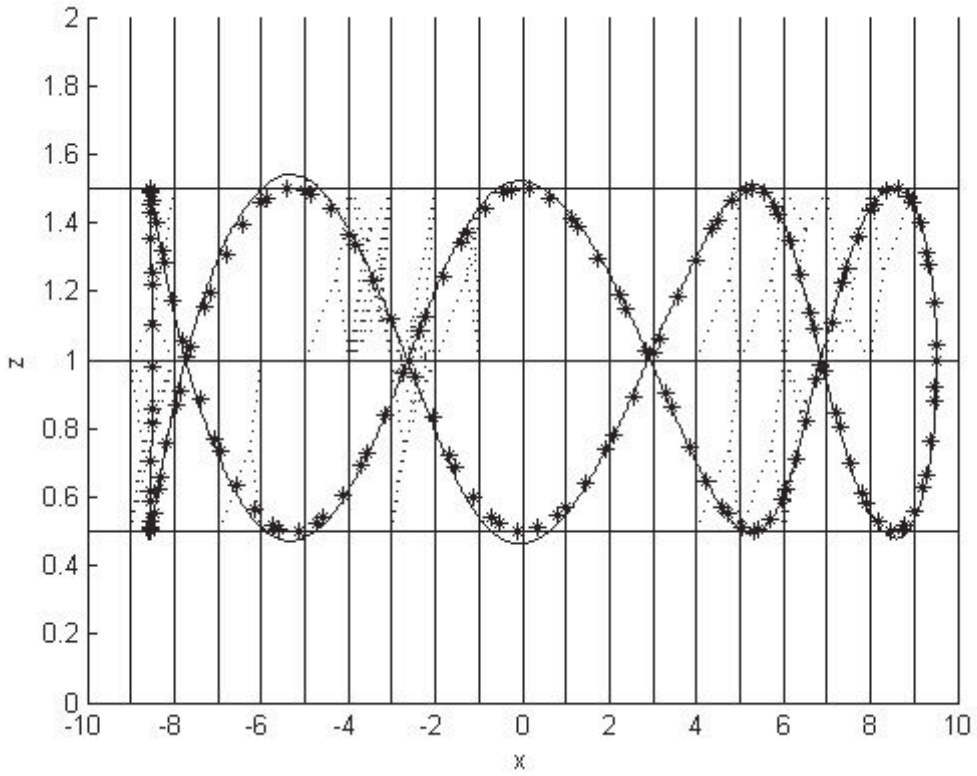

Fig. 4.21 An (*x*, *z*) view of the torus

This plot (Fig. 4.21) shows how the accuracy of the tracked streamline in *xz* plane. The subdivisions of the tetrahedra can be clearly seen. There are only a few small regions in which the tracked and exact streamlines have some slight differences.

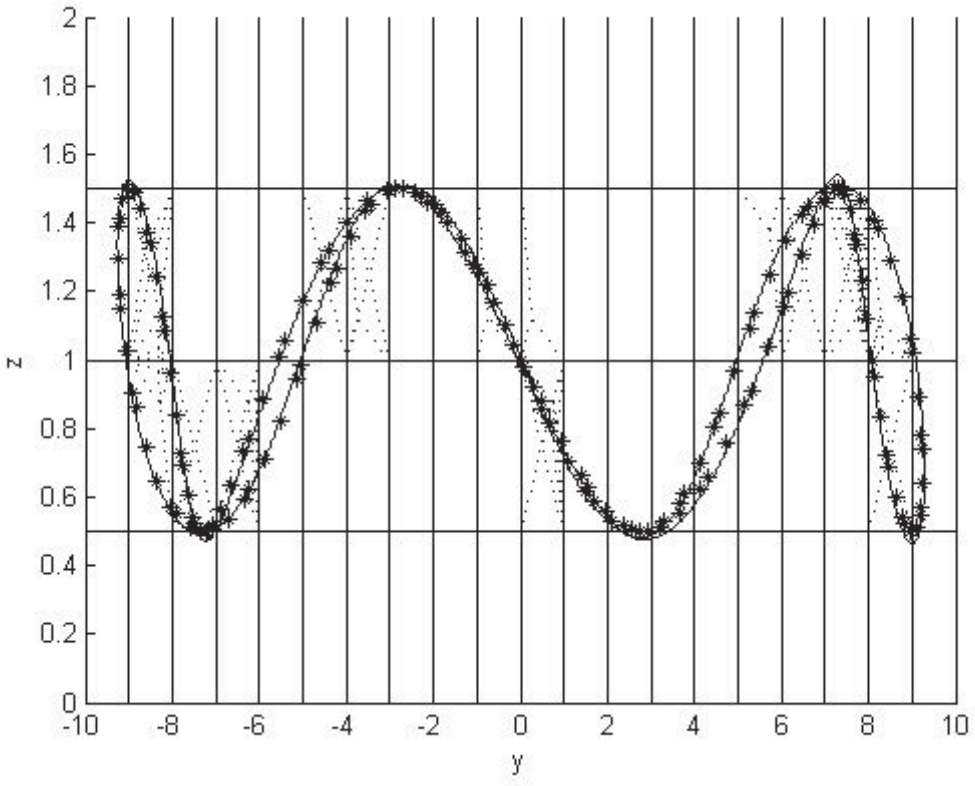

Fig. 4.22 A (y, z) view of the torus

There is a major difference between the (x, z) and (y, z) plots. In Fig. 4.21, we can see some differences between exact and tracked streamlines. In Fig. 4.22, the margin of error is very low. It seems that at most points the two streamlines coincide.

4.3 Summary

The streamline tracking method introduced in this chapter can be used only to CFD velocity fields measured by devices. No further data of velocity fields are available except for steady flows. As shown in [3, 4, 5, 7], the introduced method satisfies the law of mass conservation and it produces more accurate streamlines than those methods that do not conserve the law. This section also shows that the smaller the size of

hexahedra, the more accurate the tracked streamlines are. For a given accuracy, it is impossible to know the right size of a mesh for a velocity field before measurement. It is also expensive to have a uniform size for all cells in a mesh. Li [8, 9] describe the adaptive mesh refinement methods for both two- and three- dimensional velocity fields which further data are available such as the CFD velocity fields are numerical solutions of mathematical models. These methods provide dense nodes in the regions where the structure of velocity fields is complex.

Discussion and Future Work

This research has simplified an existing streamline tracking method for three-dimensional CFD velocity fields without further data available. Examples have shown that the tracked streamlines are accurate using this method. The overall accuracy of tracked streamline depended on the size of the hexahedrons.

These streamlines will help scientists or engineers to analyse the properties of fluid flows. Based on this method, streamtube and streamribbon can be generated to show the expansion and rotation of fluid flows.

The streamlines shown in this thesis were effectively generated using Matlab programming. The formulae were applied to steps to facilitate the generation. It consists of many small routines and requires good visual memory because of the high computational demand.

The error in the streamline tracking is a function of the cell size and aspect ratio from the examples. Even we use same cell size and aspect ratio, different velocity fields may show different errors. Some velocity field data may lead to infinite regression or to an unstable process. We can introduce a threshold number T as in [8, 9] to confine the process to finite but this would lead bigger error. These are my future research topics.

Appendix 1

Case	Eigenvalues	Expressions of tangent curves
1	$r_1 = r_2 = r_3$	$\mathbf{P}_c = \left(\mathbf{A}^{-1}\right)\left(-\mathbf{B}\right)$ $\mathbf{E}_1 = \left(\frac{\mathbf{A}-r_1\mathbf{I}}{r_1-r_2}\right)\left(\frac{r_3\mathbf{I}-\mathbf{A}}{r_3-r_1}\right)\left(\mathbf{P}_0-\mathbf{P}_c\right)$ $\mathbf{E}_2 = \left(\frac{\mathbf{A}-r_3\mathbf{I}}{r_2-r_3}\right)\left(\frac{r_2\mathbf{I}-\mathbf{A}}{r_1-r_2}\right)\left(\mathbf{P}_0-\mathbf{P}_c\right)$ $\mathbf{E}_3 = \left(\frac{\mathbf{A}-r_1\mathbf{I}}{r_3-r_1}\right)\left(\frac{r_2\mathbf{I}-\mathbf{A}}{r_2-r_3}\right)\left(\mathbf{P}_0-\mathbf{P}_c\right)$ The tangent curve is: $\mathbf{P}_b = \mathbf{E}_1 e^{(r_1 t)} + \mathbf{E}_2 e^{(r_2 t)} + \mathbf{E}_3 e^{(r_3 t)} + \mathbf{P}_c$
2 (i)	$r_1 \neq 0,$ $r_2 = r_3 \neq 0$	$\mathbf{P}_c = \left(\mathbf{A}^{-1}\right)\left(-\mathbf{B}\right)$ $\mathbf{E}_1 = \left(\frac{\mathbf{A}-r_2\mathbf{I}}{r_2-r_1}\right)^2\left(\mathbf{P}_0-\mathbf{P}_c\right)$ $\mathbf{E}_2 = \left(\frac{\left(r_1\mathbf{I}-\mathbf{A}\right)\left(r_1\mathbf{I}-2r_2\mathbf{I}+\mathbf{A}\right)}{\left(r_2-r_1\right)^2}\right)\left(\mathbf{P}_0-\mathbf{P}_c\right)$ $\mathbf{E}_3 = \left(\frac{\left(\mathbf{A}-r_1\mathbf{I}\right)\left(\mathbf{A}-r_2\mathbf{I}\right)}{\left(r_2-r_1\right)^2}\right)\left(\mathbf{P}_0-\mathbf{P}_c\right)$ The tangent curve is: $\mathbf{P}_b = \mathbf{E}_1 e^{(r_1 t)} + \mathbf{E}_2 e^{(r_2 t)} + \mathbf{E}_3 e^{(r_3 t)} + \mathbf{P}_c$
2(ii)	$r_2 \neq 0,$ $r_1 = r_3 \neq 0$	$\mathbf{P}_c = \left(\mathbf{A}^{-1}\right)\left(-\mathbf{B}\right)$ $\mathbf{E}_1 = \left(\frac{\left(r_2\mathbf{I}-\mathbf{A}\right)\left(r_2\mathbf{I}-2r_1\mathbf{I}+\mathbf{A}\right)}{\left(r_1-r_2\right)^2}\right)\left(\mathbf{P}_0-\mathbf{P}_c\right)$ $\mathbf{E}_2 = \left(\frac{\left(\mathbf{A}-r_2\mathbf{I}\right)}{\left(r_1-r_2\right)^2}\right)\left(\mathbf{P}_0-\mathbf{P}_c\right)$ $\mathbf{E}_3 = \left(\frac{\left(\mathbf{A}-r_2\mathbf{I}\right)\left(\mathbf{A}-r_1\mathbf{I}\right)}{\left(r_1-r_2\right)^2}\right)\left(\mathbf{P}_0-\mathbf{P}_c\right)$ The tangent curve is: $\mathbf{P}_b = \mathbf{E}_1 e^{(r_1 t)} + \mathbf{E}_2 e^{(r_2 t)} + \mathbf{E}_3 e^{(r_3 t)} + \mathbf{P}_c$

2(iii)	$r_1 = r_2 \neq 0,$ $r_3 \neq 0$	$$\mathbf{P}_c = \left(\mathbf{A}^{-1}\right)\left(-\mathbf{B}\right)$$ $$\mathbf{E}_1 = \left(\frac{\left(r_3\mathbf{I}-\mathbf{A}\right)\left(r_3\mathbf{I}-2r_2\mathbf{I}+\mathbf{A}\right)}{\left(r_2-r_3\right)^2}\right)\left(\mathbf{P}_0-\mathbf{P}_c\right)$$ $$\mathbf{E}_2 = \left(\frac{\left(\mathbf{A}-r_3\mathbf{I}\right)\left(\mathbf{A}-r_2\mathbf{I}\right)}{\left(r_3-r_2\right)^2}\right)\left(\mathbf{P}_0-\mathbf{P}_c\right)$$ $$\mathbf{E}_3 = \left(\frac{\mathbf{A}-r_2\mathbf{I}}{r_3-r_2}\right)^2\left(\mathbf{P}_0-\mathbf{P}_c\right)$$ The tangent curve is: $\mathbf{P}_b = \mathbf{E}_3 e^{(r_3 t)} + \mathbf{E}_1 e^{(r_1 t)} + \mathbf{E}_2 te^{(r_2 t)} + \mathbf{P}_c$
3	$r_1 = r_2 = r_3 \neq 0$	$$\mathbf{P}_c = \left(\mathbf{A}\right)^{-1}\left(-\mathbf{B}\right)$$ $$\mathbf{E}_1 = \mathbf{P}_0 - \mathbf{P}_c$$ $$\mathbf{E}_2 = \left(\mathbf{A}-r_1\mathbf{I}\right)\left(\mathbf{P}_0-\mathbf{P}_c\right)$$ $$\mathbf{E}_3 = \frac{\left(\mathbf{A}-r_1\mathbf{I}\right)^2}{2}\left(\mathbf{P}_0-\mathbf{P}_c\right)$$ The tangent curve is: $\mathbf{P}_b = \mathbf{E}_1 e^{(r_1 t)} + \mathbf{E}_2 te^{(r_1 t)} + \mathbf{E}_3 t^2 e^{(r_1 t)} + \mathbf{P}_c$
4 (i)	$r_1 = \mu_1 + \lambda_1 i,$ $r_2 = \mu_2 + \lambda_2 i,$ $r_3 = \mu_3$	$$\mathbf{P}_c = \left(\mathbf{A}^{-1}\right)\left(-\mathbf{B}\right)$$ $$\mathbf{E}_1 = \frac{\left(\mu_3\mathbf{I}-\mathbf{A}\right)\left(\mu_3\mathbf{I}-2\mu_1\mathbf{I}+\mathbf{A}\right)}{\left(\left(\mu_1-\mu_3\right)^2+\lambda_1^2\right)}\left(\mathbf{P}_0-\mathbf{P}_c\right)$$ $$\mathbf{E}_2 = \frac{\left(\mathbf{A}-\mu_3\mathbf{I}\right)\left(\left(\mathbf{A}-\mu_1\mathbf{I}\right)\left(\mu_1-\mu_3\right)+\lambda_1^2\mathbf{I}\right)}{\left(\mu_1-\mu_3\right)^2+\lambda_1^2}\left(\mathbf{P}_0-\mathbf{P}_c\right)$$ $$\mathbf{E}_3 = \frac{\left(\mathbf{A}-\mu_1\mathbf{I}\right)^2+\lambda_1^2\mathbf{I}}{\left(\left(\mu_1-\mu_3\right)^2+\lambda_1^2\right)}\left(\mathbf{P}_0-\mathbf{P}_c\right)$$ The tangent curve is: $\mathbf{P}_b = \mathbf{E}_1 e^{(\mu_1 t)}\mathbf{cos}\left(\lambda_1 t\right) + \mathbf{E}_1 e^{(\mu_1 t)}\mathbf{sin}\left(\lambda_1 t\right) + \mathbf{E}_3 e^{(\mu_3 t)} + \mathbf{P}_c$

4 (ii)	$r_1 = \mu_1 + \lambda_1 i,$ $r_2 = \mu_2,$ $r_3 = \mu_3 + \lambda_3 i$	$$\mathbf{P}_c = \left(\mathbf{A}^{-1}\right)\left(-\mathbf{B}\right)$$ $$\mathbf{E}_1 = \frac{\left(\mu_2 \mathbf{I} - \mathbf{A}\right)\left(\mu_2 \mathbf{I} - 2\mu_1 \mathbf{I} + \mathbf{A}\right)}{\left(\mu_1 + \mu_1\right)^2 + \lambda_1^2}\left(\mathbf{P}_0 - \mathbf{P}_c\right)$$ $$\mathbf{E}_2 = \frac{\left(\mathbf{A} - \mu_1 \mathbf{I}\right)^2 + \lambda_1^2 \mathbf{I}}{\left(\mu_1 + \mu_1\right)^2 + \lambda_1^2}\left(\mathbf{P}_0 - \mathbf{P}_c\right)$$ $$\mathbf{E}_3 = \frac{\left(\mathbf{A} - \mu_2 \mathbf{I}\right)\left(\left(\mathbf{A} - \mu_1 \mathbf{I}\right)\left(\mu_1 - \mu_2\right) + \lambda_1^2 \mathbf{I}\right)}{\lambda_1\left(\left(\mu_1 - \mu_2\right)^2 + \lambda_1^2\right)}\left(\mathbf{P}_0 - \mathbf{P}_c\right)$$ The tangent curve is: $\mathbf{P}_b = \mathbf{E}_1 e^{\mu_1 t}\,\mathbf{cos}\left(\lambda_1 t\right) + \mathbf{E}_3 e^{(\mu_1 t)}\,\mathbf{sin}\left(\lambda_1 t\right) + \mathbf{E}_2 e^{(\mu_1 t)} + \mathbf{P}_c$
4(iii)	$r_1 = \mu_1$ $r_2 = \mu_2 + \lambda_2 i,$ $r_3 = \mu_3 + \lambda_3 i$	$$\mathbf{P}_c = \left(\mathbf{A}^{-1}\right)\left(-\mathbf{B}\right)$$ $$\mathbf{E}_1 = \frac{\left(\mathbf{A} - \mu_2 \mathbf{I}\right)^2 + \lambda_2^2 \mathbf{I}}{\left(\mu_2 - \mu_1\right)^2 + \lambda_2^2}\left(\mathbf{P}_0 - \mathbf{P}_c\right)$$ $$\mathbf{E}_2 = \frac{\left(\mu_1 \mathbf{I} - \mathbf{A}\right)\left(\mu_1 \mathbf{I} - 2\mu_2 \mathbf{I} + \mathbf{A}\right)}{\left(\mu_2 - \mu_1\right)^2 + \lambda_2^2}\left(\mathbf{P}_0 - \mathbf{P}_c\right)$$ $$\mathbf{E}_3 = \frac{\left(\mathbf{A} - \mu_1 \mathbf{I}\right)\left(\left(\mathbf{A} - \mu_2 \mathbf{I}\right)\left(\mu_2 - \mu_1\right) + \left(\lambda_2^2 \mathbf{I}\right)\right)}{\lambda_2\left(\left(\mu_2 - \mu_1\right)^2 + \lambda_2^2\right)}\left(\mathbf{P}_0 - \mathbf{P}_c\right)$$ The tangent curve is: $\mathbf{P}_b = \mathbf{E}_2 e^{(\mu_2 t)}\,\mathbf{cos}\left(\lambda_1 t\right) + \mathbf{E}_3 e^{(\mu_2 t)}\,\mathbf{sin}\left(\lambda_2 t\right) + \mathbf{E}_1 e^{(\mu_1 t)} + \mathbf{P}_c$
5 (i)	$r_1 = 0,$ $r_2 \neq 0, r_3 \neq 0,$ $r_2 \neq r_3$	$$\mathbf{E}_1 = \left(\left(\frac{\mathbf{A} - r_3 \mathbf{I}}{\left(r_2 - r_3\right)}\right)\left(\mathbf{I} - \frac{\mathbf{A}}{r_2}\right) + \left(\frac{r_2 \mathbf{I} - \mathbf{A}}{\left(r_2 - r_3\right)}\right)\left(\mathbf{I} - \frac{\mathbf{A}}{r_3}\right)\right)\mathbf{B}$$ $$\mathbf{E}_2 = \left(\frac{\mathbf{A} - r_3 \mathbf{I}}{r_2 - r_3}\right)\left(\frac{\mathbf{A}}{r_2}\right)\left(\mathbf{P}_0 + \frac{\mathbf{B}}{r_2}\right)$$ $$\mathbf{E}_3 = \left(\frac{r_2 \mathbf{I} - \mathbf{A}}{r_2 - r_3}\right)\left(\frac{\mathbf{A}}{r_3}\right)\left(\mathbf{P}_0 + \frac{\mathbf{B}}{r_3}\right)$$ The tangent curve is: $\mathbf{P}_b = \mathbf{E}_1 t + \mathbf{E}_2\left(e^{(r_2 t)} - 1\right) + \mathbf{E}_3\left(e^{r_3 t} - 1\right) + \mathbf{P}_0$

5(ii)	$r_1 \neq 0,$ $r_2 = 0,$ $r_3 \neq 0, r_1 \neq r_3$	$$\mathbf{E}_1 = \left(\frac{\mathbf{A}-r_3\mathbf{I}}{r_1-r_3}\right)\left(\frac{\mathbf{A}}{r_1}\right)\left(\mathbf{P}_0+\frac{\mathbf{B}}{r_1}\right)$$ $$\mathbf{E}_2 = \left(\left(\frac{\mathbf{A}-r_3\mathbf{I}}{(r_1-r_3)}\right)\left(\mathbf{I}-\frac{\mathbf{A}}{r_1}\right)+\left(\frac{r_2\mathbf{I}-\mathbf{A}}{(r_1-r_3)}\right)\left(\mathbf{I}-\frac{\mathbf{A}}{r_3}\right)\right)\mathbf{B}$$ $$\mathbf{E}_3 = \left(\frac{r_1\mathbf{I}-\mathbf{A}}{r_1-r_3}\right)\left(\frac{\mathbf{A}}{r_3}\right)\left(\mathbf{P}_0+\frac{\mathbf{B}}{r_3}\right)$$ The tangent curve is: $\mathbf{P}_b = \mathbf{E}_2 t + \mathbf{E}_1\left(e^{(r_1 t)}-1\right)+\mathbf{E}_3\left(e^{r_3 t}-1\right)+\mathbf{P}_0$
5(iii)	$r_1 \neq 0,$ $r_2 \neq 0,$ $r_3 = 0, r_1 \neq r_2$	$$\mathbf{E}_1 = \left(\frac{\mathbf{A}-r_2\mathbf{I}}{r_1-r_2}\right)\left(\frac{\mathbf{A}}{r_1}\right)\left(\mathbf{P}_0+\frac{\mathbf{B}}{r_1}\right)$$ $$\mathbf{E}_2 = \left(\frac{r_1\mathbf{I}-\mathbf{A}}{r_1-r_2}\right)\left(\frac{\mathbf{A}}{r_2}\right)\left(\mathbf{P}_0+\frac{\mathbf{B}}{r_2}\right)$$ $$\mathbf{E}_3 = \left(\left(\frac{\mathbf{A}-r_2\mathbf{I}}{(r_1-r_2)}\right)\left(\mathbf{I}-\frac{\mathbf{A}}{r_1}\right)+\left(\frac{r_2\mathbf{I}-\mathbf{A}}{(r_1-r_2)}\right)\left(\mathbf{I}-\frac{\mathbf{A}}{r_2}\right)\right)\mathbf{B}$$ The tangent curve is: $\mathbf{P}_b = \mathbf{E}_3 t + \mathbf{E}_1\left(e^{(r_1 t)}-1\right)+\mathbf{E}_3\left(e^{r_2 t}-1\right)+\mathbf{P}_0$
6 (i)	$r_1 = r_2 = 0,$ $r_3 \neq 0$	$$\mathbf{E}_1 = \mathbf{A}\,\mathbf{P}_0+\mathbf{B}$$ $$\mathbf{E}_2 = \left(\mathbf{I}-\frac{\mathbf{A}}{r_3}\right)\frac{\mathbf{AB}}{2}$$ $$\mathbf{E}_3 = \left(\frac{\mathbf{A}}{r_3}\right)^2\left(\mathbf{P}_0+\frac{\mathbf{B}}{r_3}\right)$$ The tangent curve is: $\mathbf{P}_b = \mathbf{E}_1 t + \mathbf{E}_2 t^2 + \mathbf{E}_3\left(\left(e^{r_3 t}-1\right)-r_3 t-1\right)+\mathbf{P}_0$
6(ii)	$r_1 = r_3 = 0,$ $r_2 \neq 0$	$$\mathbf{E}_1 = \left(\frac{\mathbf{A}}{r_1}\right)^2\left(\mathbf{P}_0+\frac{\mathbf{B}}{r_1}\right)$$ $$\mathbf{E}_2 = \mathbf{A}\mathbf{P}_0+\mathbf{B}$$ $$\mathbf{E}_3 = \left(\mathbf{I}-\frac{\mathbf{A}}{r_1}\right)\frac{\mathbf{AB}}{2}$$ The tangent curve is: $\mathbf{P}_b = \mathbf{E}_2 t + \mathbf{E}_3 t^2 + \mathbf{E}_1\left(\left(e^{r_1 t}-1\right)-r_1 t-1\right)+\mathbf{P}_0$

7	$r_1 = r_2 = r_3 = 0$	$\mathbf{E}_1 = \mathbf{A}\,\mathbf{P}_0 + \mathbf{B}$ $\mathbf{E}_2 = \frac{\mathbf{A}}{2}\left(\mathbf{A}\mathbf{P}_0 + \mathbf{B}\right)$ $\mathbf{E}_3 = \mathbf{A}^2\frac{\mathbf{B}}{6}$ The tangent curve is: $\mathbf{P}_b = \mathbf{E}_1 t + \mathbf{E}_2 t^2 + \mathbf{E}_3 t^3 + \mathbf{P}_0$
8 (i)	$r_1 = 0,$ $r_2 \neq 0,$ $r_3 \neq 0,$ $r_2 = r_3$	$\mathbf{E}_1 = \left(\left(\mathbf{I} + \frac{\mathbf{A}}{r_3}\right)\left(\frac{\mathbf{A}}{r_3} - 2\mathbf{I}\right)\right)\mathbf{B}$ $\mathbf{E}_2 = \frac{\mathbf{A}}{r_3}\left(2\left(\mathbf{I} - \frac{\mathbf{A}}{r_3}\right)\left(\mathbf{P}_0 + \frac{\mathbf{B}}{r_3}\right) + \frac{\mathbf{A} + \mathbf{P}_0 + \mathbf{B}}{r_3}\right)$ $\mathbf{E}_3 = \mathbf{A}\left(\frac{\mathbf{A}}{r_3} - \mathbf{I}\right)\left(\mathbf{P}_0 + \frac{\mathbf{B}}{r_3}\right)$ The tangent curve is: $\mathbf{P}_b = \mathbf{E}_1 t + \mathbf{E}_2\left(e^{(r_3 t)} - 1\right) + \mathbf{E}_3 t e^{(r_3 t)} + \mathbf{P}_0$
8(ii)	$r_1 \neq 0,$ $r_2 = 0,$ $r_3 \neq 0,$ $r_1 = r_3$	$\mathbf{E}_1 = \frac{\mathbf{A}}{r_3}\left(2\left(\mathbf{I} - \frac{\mathbf{A}}{r_3}\right)\left(\mathbf{P}_0 + \frac{\mathbf{B}}{r_3}\right) + \frac{\mathbf{A} + \mathbf{P}_0 + \mathbf{B}}{r_3}\right)$ $\mathbf{E}_2 = \left(\left(\mathbf{I} + \frac{\mathbf{A}}{r_3}\right)\left(\frac{\mathbf{A}}{r_3} - 2\mathbf{I}\right)\right)\mathbf{B}$ $\mathbf{E}_3 = \mathbf{A}\left(\frac{\mathbf{A}}{r_3} - \mathbf{I}\right)\left(\mathbf{P}_0 + \frac{\mathbf{B}}{r_3}\right)$ The tangent curve is: $\mathbf{P}_b = \mathbf{E}_2 t + \mathbf{E}_1\left(e^{(r_3 t)} - 1\right) + \mathbf{E}_3 t e^{(r_3 t)} + \mathbf{P}_0$
8(iii)	$r_1 \neq 0,$ $r_2 \neq 0,$ $r_3 = 0,$ $r_1 = r_2$	$\mathbf{E}_1 = \left(\left(\mathbf{I} + \frac{\mathbf{A}}{r_1}\right)\left(\frac{\mathbf{A}}{r_1} - 2\mathbf{I}\right)\right)\mathbf{B}$ $\mathbf{E}_2 = \frac{\mathbf{A}}{r_1}\left(2\left(\mathbf{I} - \frac{\mathbf{A}}{r_1}\right)\left(\mathbf{P}_0 + \frac{\mathbf{B}}{r_1}\right) + \frac{\mathbf{A} + \mathbf{P}_0 + \mathbf{B}}{r_1}\right)$ $\mathbf{E}_3 = \mathbf{A}\left(\frac{\mathbf{A}}{r_1} - \mathbf{I}\right)\left(\mathbf{P}_0 + \frac{\mathbf{B}}{r_1}\right)$ The tangent curve is: $\mathbf{P}_b = \mathbf{E}_3 t + \mathbf{E}_1\left(e^{(r_1 t)} - 1\right) + \mathbf{E}_2 t e^{(r_1 t)} + \mathbf{P}_0$

9 (i)	$r_1 = \mu_1 + \lambda_1 i,$ $r_2 = \mu_2 + \lambda_2 i,$ $r_3 = 0$	$\mathbf{E}_1 = \left(\frac{\mathbf{A}}{\mu_1^2+\lambda_1^2}\right)\left((2\mu_1\mathbf{I}-\mathbf{A})\mathbf{P}_0+\left(\frac{3\mu_1^2\mathbf{I}-\lambda_1^2\mathbf{I}-2\mu_1\mathbf{A}}{\mu_1^2+\lambda_1^2}\right)\mathbf{B}\right)$ $\mathbf{E}_2 = \left(\frac{\mathbf{A}}{\lambda_1(\mu_1^2+\lambda_1^2)}\right)\left(\mu_1\mathbf{A}-(\mu_1^2-\lambda_1^2)\mathbf{I}\right)\mathbf{P}_0+(\mu_1^2+\lambda_1^2)\mathbf{A}-\left(\frac{\mu_1(\mu_1^2-3\lambda_1^2)\mathbf{I}}{\mu_1^2+\lambda_1^2}\right)\mathbf{B}$ $\mathbf{E}_3 = \left(\mathbf{I}-\mathbf{A}\left(\frac{2\mu_1\mathbf{I}-\mathbf{A}}{\mu_1^2+\lambda_1^2}\right)\right)\mathbf{B}$ The tangent curve is: $\mathbf{P}_b = \mathbf{E}_1\left(e^{(\mu_1 t)}\cos(\lambda_1 t)-1\right)+\mathbf{E}_2 e^{(\mu_1 t)}\sin(\lambda_1 t)+\mathbf{E}_3 t+\mathbf{P}_0$
9(ii)	$r_1 = \mu_1 + \lambda_1 i,$ $r_2 = 0$ $r_3 = \mu_3 + \lambda_3 i,$	$\mathbf{E}_1 = \left(\frac{\mathbf{A}}{\mu_1^2+\lambda_1^2}\right)\left((2\mu_1\mathbf{I}-\mathbf{A})\mathbf{P}_0+\left(\frac{3\mu_1^2\mathbf{I}-\lambda_1^2\mathbf{I}-2\mu_1\mathbf{A}}{\mu_1^2+\lambda_1^2}\right)\mathbf{B}\right)$ $\mathbf{E}_2 = \left(\mathbf{I}-\mathbf{A}\left(\frac{2\mu_1\mathbf{I}-\mathbf{A}}{\mu_1^2+\lambda_1^2}\right)\right)\mathbf{B}$ $\mathbf{E}_3 = \left(\frac{\mathbf{A}}{\lambda_1(\mu_1^2+\lambda_1^2)}\right)\left(\mu_1\mathbf{A}-(\mu_1^2-\lambda_1^2)\mathbf{I}\right)\mathbf{P}_0+(\mu_1^2+\lambda_1^2)\mathbf{A}-\left(\frac{\mu_1(\mu_1^2-3\lambda_1^2)\mathbf{I}}{\mu_1^2+\lambda_1^2}\right)\mathbf{B}$ The tangent curve is: $\mathbf{P}_b = \mathbf{E}_1\left(e^{(\mu_1 t)}\cos(\lambda_1 t)-1\right)+\mathbf{E}_3 e^{(\mu_1 t)}\sin(\lambda_1 t)+\mathbf{E}_2 t+\mathbf{P}_0$
9(iii)	$r_1 = 0,$ $r_2 = \mu_2 + \lambda_2 i,$ $r_3 = \mu_3 + \lambda_3 i,$	$\mathbf{E}_1 = \left(\mathbf{I}-\mathbf{A}\left(\frac{2\mu_1\mathbf{I}-\mathbf{A}}{\mu_2^2+\lambda_2^2}\right)\right)\mathbf{B}$ $\mathbf{E}_2 = \left(\frac{\mathbf{A}}{\mu_2^2+\lambda_2^2}\right)\left((2\mu_2\mathbf{I}-\mathbf{A})\left(\frac{3\mu_2^2\mathbf{I}-\lambda_2^2\mathbf{I}-2\mu_2\mathbf{A}}{\mu_2^2+\lambda_2^2}\right)\mathbf{B}\right)$ $\mathbf{E}_3 = \left(\frac{\mathbf{A}}{\lambda_2(\mu_2^2+\lambda_2^2)}\right)\left(\mu_2\mathbf{A}-(\mu_2^2-\lambda_2^2)\mathbf{I}\right)\mathbf{P}_0+(\mu_2^2+\lambda_2^2)\mathbf{A}-\left(\frac{\mu_2(\mu_2^2-3\lambda_2^2)\mathbf{I}}{\mu_2^2+\lambda_2^2}\right)\mathbf{B}$ The tangent curve is: $\mathbf{P}_b = \mathbf{E}_1\left(e^{(\mu_2 t)}\cos(\lambda_2 t)-1\right)+\mathbf{E}_3 e^{(\mu_2 t)}\sin(\lambda_2 t)+\mathbf{E}_2 t+\mathbf{P}_0$

Table 2 Jacobeans and expressions of f for all possible cases of a non-conservative 3D linear field (where C is a constant)

Case	Jacobean	f
1	$\begin{pmatrix} r_1 & 0 & 0 \\ 0 & r_2 & 0 \\ 0 & 0 & r_3 \end{pmatrix}$ $(0 \neq r_1 \neq r_2 \neq r_3 \neq 0)$	$\left(y_1 + \frac{b_1}{r_1}\right)^{-1}\left(y_2 + \frac{b_2}{r_2}\right)^{-1}\left(y_3 + \frac{b_3}{r_3}\right)^{-1}$
2	$\begin{pmatrix} \mu & \lambda & 0 \\ -\lambda & \mu & 0 \\ 0 & 0 & r \end{pmatrix}$ $(r \neq 0, \lambda \neq 0)$	$\left\{\left(y_1 + \frac{\mu b_1 - \lambda b_2}{\mu^2 + \lambda^2}\right)^2 + \left(y_2 + \frac{\lambda b_1 + \mu b_2}{\mu^2 + \lambda^2}\right)^2\right\}^{-1}\left(y_3 + \frac{b_3}{r}\right)^{-1}$
3	$\begin{pmatrix} a & \delta & 0 \\ 0 & a & 0 \\ 0 & 0 & r \end{pmatrix}$ $(a \neq 0, r \neq 0)$ $(\delta = 0 \text{ or } 1)$	$\left(y_2 + \frac{b_2}{a}\right)^{-2}\left(y_3 + \frac{b_3}{r}\right)^{-1}$
4	$\begin{pmatrix} \mu & \lambda & 0 \\ -\lambda & \mu & 0 \\ 0 & 0 & 0 \end{pmatrix}$ $(\lambda \neq 0)$	$\left\{\left(y_1 + \frac{\mu b_1 - \lambda b_2}{\mu^2 + \lambda^2}\right)^2 + \left(y_2 + \frac{\lambda b_1 + \mu b_2}{\mu^2 + \lambda^2}\right)^2\right\}^{-1}$

5	$\begin{pmatrix} r & \delta & 0 \\ 0 & r & 0 \\ 0 & 0 & 0 \end{pmatrix}$ $(r \neq 0, \delta = 0 \text{ or } 1)$	$\left(y_2 + \frac{b_2}{r}\right)^{-2}$
6	$\begin{pmatrix} r & \delta & 0 \\ 0 & r & \delta \\ 0 & 0 & r \end{pmatrix}$ $(r \neq 0, \delta = 0 \text{ or } 1)$	$\left(y_3 + \frac{b_3}{r}\right)^{-3}$
7	$\begin{pmatrix} r & 0 & 0 \\ 0 & 0 & \delta \\ 0 & 0 & 0 \end{pmatrix}$ $(r \neq 0, \delta = 0 \text{ or } 1)$	$\left(y_1 + \frac{b_1}{r}\right)^{-1}$
8	$\begin{pmatrix} r_1 & 0 & 0 \\ 0 & r_2 & 0 \\ 0 & 0 & 0 \end{pmatrix}$ $(0 \neq r_1 \neq r_2 \neq 0)$	$\left(y_1 + \frac{b_1}{r_1}\right)^{-1}\left(y_2 + \frac{b_2}{r_2}\right)^{-1}$

References

[1] Feng, D., Wang, X., Cai, W., Shi, J., 1997, "A Mass Conservative Flow Field Visualization Method", *Computers & Graphics*, vol. 21(6), pp. 749-756.

[2] Knight, D., and Mallinson, G. D., 1996, “Visualising Unstructured Flow Data Using Dual Stream Functions,” *IEEE Trans. on Visualization and Computer Graphics*, Vol. 2, pp. 355-363.

[3] Li, Z., and Mallinson, G.D., 2001, “Mass Conservative Fluid Flow Visualization for CFD Velocity fields”, *KSME International Journal*, Vol. 15, pp. 1794-1800.

[4] Li, Z., 2002, “Mass Conservative Streamline Tracking Method for Two Dimensional CFD Velocity fields”, *Journal of flow visualization and image processing*, Vol. 9, pp.75-87.

[5] Li, Z., 2002, “Tangent Curves for linearly varying Conservative Vector Fields over tetrahedral domains”, *Proceedings of image and Vision Computing New Zealand 2002*, Auckland, New Zealand, pp.35-38.

[6] Li, Z., 2003, "A Mass conservative streamline tracking method for Three dimensional CFD velocity fields", *Proceedings of FEDSM’03 (4TH ASME_JSME Joint Fluids Engineering Conference),* FEDSM2003-45526, Honolulu, Hawaii, USA.

[7] Li, Z., Mallinson, G., 2004, "Simplifications of An Existing Mass Conservative Streamline Tracking Method for 2D CFD Velocity Fields", *GIS and Remote Sensing in*

Hydrology, Water Resources and Environment, Yangbo Chen, Kaoru Takara, Ian D. Cluckies & F. Hilaire De Smedt, eds. IAHS Press, 289, pp. 269-275.

[8] Li, Z., 2007, “An adaptive three-dimensional mesh refinement method based on the law of mass conservation”, *Journal of Flow Visualization and Image Processing,* 14(4), 375-395.

[9] Li, Z., 2008, “An adaptive two-dimensional mesh refinement method based on the law of mass conservation”, *Journal of Flow Visualization and Image Processing*, 15(1), 17-33.

[10] Nielson, G. M., Jung, I.-H., 1999, "Tools for Computing Tangent Curves for Linearly Varying Vector Fields over Tetrahedral Domains", *IEEE Trans. on Visualization and Computer Graphics,* vol. 5(4), pp. 360-372.

[11] Nielson, G. M, 1997, “Tools for Triangulations and Tetrahedrization and Construction Functions Defined over Them”, *Scientific Visualization: Overviews, Methodologies, and Techniques,* G. M Nielson, H. Hagen, and H. Mueller, eds., pp. 429-526, IEEE CS Press.

[12] Singh R. P., and Li, Z., 2007, “A Mass Conservative Streamline Tracking Method for Three Dimensional CFD Velocity Fields”. *J. of Flow Visualization and Image Processing, Vol.* 14, pp. 107-120.

[13] Yeung, P. K., and Pope, S. B, 1988, "An Algorithm for Tacking Fluid Particles in Numerical Simulations of Homogeneous Turbulence", *J. Computational Physics,* vol. 79, pp. 373-416.